Journal of the Geological Survey of Brazil

Geological characteristics of the Serra do Navio Formation, Guiana Shield, Brazil, and its manganiferous ores: queluzite as a source rock of oxide and carbonate manganese ores

Wilson Scarpelli

Independent Consultant, Rua da Paz 119, Cotia-SP, Brazil, CEP: 06710-507

Abstract

The Serra do Navio manganese deposit in the Amapá State, Eastern Guiana Shield, northernmost Brazil, had its reserves of high-grade oxide ores exhausted, after the production of 33 million tonnes, assaying more than 45% Mn. However, possibly with greater tonnages, the carbonatic protores, the queluzites, remain practically intact, available for exploration and mining. The queluzites occur as lenses, in the upper part of each cycle of the metamorphosed megacyclothem that constitutes the Serra do Navio Formation. Each cycle initiates with sediments of a marine near-littoral quartzose facies, represented by metamorphosed limestones, cherts, and silts, overlain by an intermediate argillaceous, now biotitic, facies, and closing up with a coastal organic material-rich clay, now graphitic, facies, host of lenses of manganese carbonates, now queluzites. The sequence was metamorphosed on three occasions. The first was regional, with folds verging to the north-northeast. The second was thermal, marked by porphyroblasts as diopside, andalusite, staurolite, cordierite, sillimanite, almandine, spessartite, picrotephroite, rhodonite and others. Some porphyroblasts preserve remnant minerals and structures of the former metamorphism. The third metamorphism was regional, with fold axis to the northwest, being marked by a shear zone causing strong deformation along its trace. Broken and displaced minerals and rock fragments occur in deformed areas. In some areas, weak retrograde metamorphism is marked by veinlets of quartz and calcite, chloritization, tourmalinization, and dispersion of iron sulfides.

Article Information

Publication type: Review article
Received 20 Setember 2021
Accepted 7 June 2022
Online pub. 24 June 2022
Editor: Abidi Riadh

Keywords:
Indicator of life,
Paleoproterozoic,
Megacyclothem,
Metamorphic superposition,
Sillimanite,
Fibrolite

*Corresponding author
Wilson Scarpelli
wiscar@terra.com.br

1. Introduction

The Serra do Navio Formation is a metasedimentary sequence that is part of greenstone belts of the Eastern Guiana Shield, in Amapá State, northernmost Brazil (Fig. 1), and host of important deposits of manganese in the form of beds of queluzites (Appendix A). The main objective of this article is the presentation of a summary of the discovery, geology and mining of the now exhausted supergene ores of manganese oxides, and to call attention to the large volumes of fresh queluzites available for the production of manganese carbonates and industrial by-products of manganese. For this purpose, it includes information and suggestions that might be used during a forthcoming exploration of the queluzites.

The article includes a review of the geology of the metamorphosed megacyclothem (Dunbar and Rodgers 1958; Duff et al. 1967 – and Appendix A) that constitutes the Serra do Navio Formation, and discusses the structural and petrographic data considered important in the studies of the local and the regional geology of the greenstones of Amapá.

1.1. Local physiography and conditions of weathering

The State of Amapá is formed by rocks of the Guiana Shield and is covered by the Amazon Rain Forest, with the exception of a border of Paleozoic to Quaternary sediments flanking the State by the littoral, at the East, and along the margin with the Amazon River, at the South (Fig. 1). Most of it is formed by a basement of Archean gneisses and granitic intrusives, which have a subdued topography, with hills of less than 80 meters of elevation above the countryside. Overlying this basement, there are belts of metamorphosed volcanic and sedimentary rocks, which are more resistant to erosion and appear as hills, ridges and plateaus, with a few hundreds of meters of elevation above the countryside, often with steep slopes at inner parts and at their edges.

ISSN: 2595-1939
https://doi.org/10.29396/jgsb.2022.v5.n2.2
Open access at jgsb.cprm.gov.br

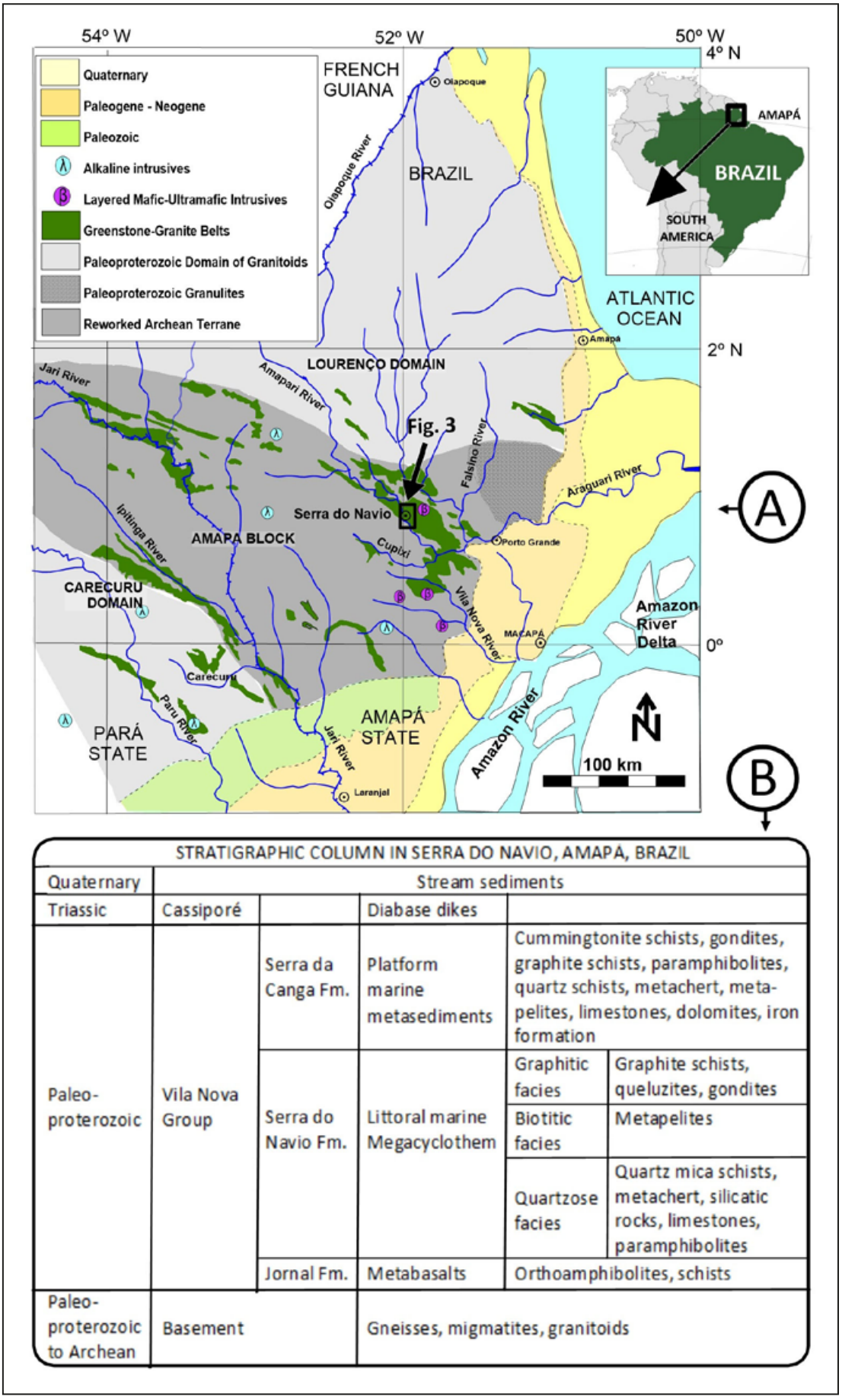

STRATIGRAPHIC COLUMN IN SERRA DO NAVIO, AMAPÁ, BRAZIL

Quaternary	Stream sediments				
Triassic	Cassiporé		Diabase dikes		
Paleo-proterozoic	Vila Nova Group	Serra da Canga Fm.	Platform marine metasediments	Cummingtonite schists, gondites, graphite schists, paramphibolites, quartz schists, metachert, meta-pelites, limestones, dolomites, iron formation	
		Serra do Navio Fm.	Littoral marine Megacyclothem	Graphitic facies	Graphite schists, queluzites, gondites
				Biotitic facies	Metapelites
				Quartzose facies	Quartz mica schists, metachert, silicatic rocks, limestones, paramphibolites
		Jornal Fm.	Metabasalts	Orthoamphibolites, schists	
Paleo-proterozoic to Archean	Basement		Gneisses, migmatites, granitoids		

FIGURE 1. (A) Location of Serra do Navio near the center of the State of Amapá, in Northern Brazil, and main geological units of Eastern Guiana Shield. (B) Stratigraphic column at Serra do Navio (details and references in the text).

The rainfall in the area varies from 2,000 to 3,000 millimeters per year, mostly concentrated from December to May, with scarce rains from October to November. Under the year-round moderate to high temperature of the Equator and the forest protection from winds and sunlight, the weathering of the rocks is essentially of a chemical nature. Due to the acids produced by litterfall decay, the water in the soil is acid, with a pH from 4.5 to 6.0. Under such low pH, combined with the high flux of rainwater, the chemical alteration of the rocks is quite intense, with solubilization and removal of most of the elements, such as calcium, magnesium, potassium and others, leaving behind only resistant minerals, such as quartz, gold, graphite, cassiterite, rutile, tantalite, and a few others, usually accompanied by clays and secondary minerals of manganese, iron, aluminum, silica, and nickel. In the ridges of Serra do Navio, weathering reaches more than 50 meters in depth in silicate rocks, and about 100 meters in depth in carbonatic rocks. In general, dissolution mostly occurs during the wet season, while the precipitation of new minerals occurs mainly in the dry seasons, caused by water losses due to evaporation and absorption by roots of the vegetation. The role of bacteria in this weathering needs to be further studied.

In addition to the chemical and mineralogical composition of the lithologies, weathering is also affected by discontinuities in the rocks, such as planes of foliation, fractures and faults, which allow water to penetrate deeper. As such, alteration is more intense in foliated rocks, such as schists and gneisses, and less intense in massive zones of igneous and metasedimentary rocks without fractures, as some portions of diabase dikes, metacherts and a few granitic intrusions. Where altered, foliated quartzites become friable, made of loose grains of quartz. Under these conditions, outcrops are scarce, and some lithologies only exceptionally outcrop.

In this environment, the ridges standing out in the relief show the most resistant lithologies, amongst which those rich in quartz, silicified zones, iron formations, and residual resistant minerals, such as the secondary oxides and hydroxides of manganese, iron, and aluminum. The soil zone A is normally thin, usually with less than 1 meter of thickness, and the soil zone B is rich in iron, forming laterite, characterized by the presence of loose millimetric to decimetric concretions of iron oxides and hydroxides, or “canga”, a hard duricrust made of concretions of iron oxides and hydroxides cemented together.

1.2. From discovery to mining of the oxide ores

Serra do Navio (Fig. 1) is situated in the State of Amapá, Brazil, Eastern Guiana Shield, approximately 190 kilometers to the northwest of Macapá, the capital of the state. Its lowest topographic feature is the Amapari River, which is about 90 meters above sea level. The area is covered by the dense Amazon Forest, and the topography is marked by ridges that reach 250 to 350 meters above sea level. Blocks of manganese oxides were first reported in 1934 by the Mining and Civil Engineer Josalfredo Borges (Ackerman 1948), of the Brazilian Mines Ministry, but the information was not followed up. In 1945, stimulated by a reward offered for samples of iron ores, which were very important in post-war years, samples of manganese oxide ores were brought to the state government by the river-merchant/hunter/fisherman Mario Cruz. Next, the samples were sent to the Departamento Nacional da Produção Mineral, where the Geologist Glycon de Paiva, and the Petrologist Evaristo Scorza described the samples as manganese ores (Ramos 1983).

Thereafter, the mineral rights were granted to the government, and a bid was opened for their exploration and exploitation. Proposals were presented by United State Steel Corp., Hanna Coal and Ore Corp., and Indústria e Comércio de Minérios Ltda., this latter being a small Brazilian miner of iron and manganese ores of Minas Gerais, owned by Augusto Trajano de Azevedo Antunes. The bid was won by the Brazilian company, which, in addition to other favorable conditions, guaranteed that the Brazilian participation in the company will always be equal to or greater than 51%, and that fieldwork would start in one year, before the end of 1948, what was effectively done. To carry out the work, the company admitted new Brazilian shareholders, increased its capital, and changed its name to Indústria e Comércio de Minérios S.A. – ICOMI (Ramos 1983).

To start, ICOMI installed a field camp on the right bank of the Amapari River, down from a high ridge, locally named “Navio” due to its similarity to a ship’s keel. This appearance was due to a cliff-like outcrop of manganese ore (Dorr II et al. 1950). This was the origin of the name Serra do Navio. This ridge was mined under the name of F-12.

ICOMI conducted a geological survey and drilling program aimed to find 10 million tonnes of oxide manganese ore, which at the time was considered to be the minimum necessary to justify the opening of a mine in that remote area.

After a few years of exploration, it was clear that the potential was considerably greater, indicating the need for a greater project. This fact led to a revision, in 1950, of the contract with the government. Among other items, the new contract defined the geographical limits of the mine concession, the areas necessary for the social and industrial activities and authorized the construction of a port, a 192- kilometers-long railway, a mining village at Serra do Navio, and other structures. The ownership of these facilities, areas and equipment would be transferred to the government after 50 years. The contract set forth the terms for the participation of a foreign company, and the guarantee of the payment of a free royalty of 3% of the gross selling values of the shipments of the ore; that is, not considering operating costs and taxes. It also established that an additional 1% could be paid either in investments in Amapá or in addition to the royalty (Ramos 1983).

After the terms set forth, ICOMI looked for a foreign partner and chose Bethlehem Steel Corp., which acquired 49% of the company. To fund the project, a loan was obtained from the Export and Import Bank of Washington (EXIMBANK). Bethlehem provided the engineering of the port, port yard, the 192-km long railway, the ore beneficiation plant in Serra do Navio, and two industrial areas, at the mine and the port areas. For the mine, a fleet of trucks, bucket excavators, scrapers, dozers and other pieces of equipment were acquired. For the employees, ICOMI built two well equipped villages at Santana and Serra do Navio, both designed by the Brazilian Engineer O.A. Bratke (Ramos 1983).

In 1953, when the industrial infrastructure was established, and the operation started, the 50-years period determined by the concession for the mining started to be counted, guaranteeing ICOMI the rights to explore the ore until 2003.

The initial years were of preparation, with ore shipment starting in 1957 (Ramos 1983).

During the life of the mine, the ores were sold to a number of steel plants, a few in Brazil, with the majority in Europe, followed by the United States and Asia. During the initial years of production, there were few competitors, and the ores of Serra do Navio represented a very important contributor to world steel production (Ramos 1983). The payment of the EXIMBANK loan was completed before the end of 1964.

The production started in the area where most of the initial reserves were identified, in the mines T-6, T-4 and T-20. The industrial area and the main offices were built in the foothill of the T-20 mine. While these mines were in operation, the geological team explored the mines to the north, looking for the identification of new reserves to replace those being mined. Slowly, mining progressed northwards, reaching the mines A-12, A-3, C-10, C-5 and C-2. At that point, a conveyor belt was built across the Amapari River and the last orebody was mined at F-12.

The mine was declared exhausted of economically minable oxide ores in 1998, after the commercialization of more than 33 million tonnes of processed and classified ores, pellets and sinter, in average assaying more than 45% Mn. During the last years of activity, the mine also exploited and sold almost 1 million tonnes of fresh queluzites assaying 32% Mn. This carbonatic ore was mined at the bottom of the cave of the F-12 mine (Costa 1997).

In 2003, after the 50 years of the concession, the state took possession of the port of Santana, the railway, and, in Serra do Navio, the village, the mine, assets of infrastructure and the industrial area. Recognizing the importance of the layout and of the features of the construction of the village, the Instituto do Patrimônio Histórico e Artístico Nacional (IPHAN – Brazilian national institute of the historical and artistic heritage), declared Serra do Navio a National Monument, to be preserved (Lima et al. 2008).

1.3. Present situation

As the mineral rights returned to the state, it has to decide what to do with the stockpiles of oxide ores left resulting from the operation and the large resources of manganese represented by the lenses of queluzites, which occur below the zone of weathering.

When the operation was completed, the remaining in situ resource of oxide ores was estimated by ICOMI to be adequate to produce, with crushing and washing, 1,164,000 tonnes at 38% Mn (Costa 1997). In 2005, during a visit, this author observed that, in addition,, the operation left a few large stockpiles of non-beneficiated low-grade ore material, that, after crushing, screening and washing, could result in at least 3,000,000 tonnes of low-grade ore products, at about 30% Mn. Unfortunately, at this moment, it is impossible to process these resources of oxide ores, since the beneficiation plant has been abandoned for many years, and some pieces of equipment were removed or are damaged.

Near the plant yard, there are 6,500,000 tonnes of stockpiled oxide ores, washed and screened, with several grain sizes and grades, and with an average grade of about 30% Mn, plus more than 6,000 tonnes of crushed and screened queluzite, assaying 31% Mn.

1.4. Oxide ore exposures, types and mineralogy

The manganese oxide ores were found along 11 kilometers of ridges oriented northwest, and crossing the Amapari River. They were observed as accumulations of loose large blocks on the surface, among a few outstanding outcrops, some reaching several meters in height and up to a few hundred of meters in extent (Fig. 2A) (Dorr II et al. 1949; Nagell and Seara 1959, Nagell 1962). Most of the blocks and the great majority of outcrops were formed by massive ore (Fig. 2B), made of very black, compact and hard manganese oxides, containing from 45 to +52% Mn (All chemical grades mentioned in this article refer to the weight percentage of the element in the total weight of the rock), and with a density above 4. Some of the loose blocks slid downhill from the outcrops, mixing with soil clays, oxides and hydroxides of iron and aluminum, forming a blanket of mineralization, reaching up to about 10 meters in thickness, forming the float ore.

A very important feature of the massive ore is the occasional presence of fresh spessartite garnet, completely surrounded by manganese oxides and preserved from weathering. They have, without exception, a diameter of less than 1 millimeter. Based on the observation that there were very few remnants of original minerals, Leinz (1948) wrote that the ore could be originated from the weathering of a rock rich in carbonates, which was proved to be correct when the first core hole reached the fresh, not oxidized, queluzite.

A characteristic of the soil in areas near the orebodies was the presence of granzon, which is an onion-like spherical concretion made of superposed sub-millimetric laminae of chemically deposited manganese, iron and aluminum oxides and hydroxides. The spherules of granzon varied from 0.5 to 1.5 centimeters in diameter, occasionally blended together (Dorr II et al. 1950; Nagell 1962). The presence of granzon in areas without outcrops of the ore was a strong lead to a non-outcropping mass of manganese oxide ore.

Two types of low-grade (below 40% Mn) ores were found. One was in the form of weathered gondites (a metamorphic rock composed of quartz, spessartite, and other manganiferous silicates), most of them at the margins of the massive ores. They are constituted by an aggregate of quartz and weathered silicates, kept together by interstitial limonite and manganese oxides and hydroxides. They are slightly porous, have a density below 3, and have grades of 28 to 36% of manganese. Quite important, the spessartite, albeit weathered, is easily identified, and has a diameter of 3 to 5 or more millimeters, much larger than the spessartite of the massive ore.

The other type of low-grade ore was made of wedges and pockets of weathered schists partially replaced by oxides and hydroxides of manganese. They were found at or near contacts of schists with the high-grade ores, along faults in zones of tectonic transposition related to shearing and folding. This schistose ore is usually made of small masses of manganese oxides mixed with clays and fine-grained quartz. It contains more iron, silica and alumina than the high-grade ore.

1.5. Formation and characteristics of the manganese oxide ores

The alteration of the minerals of the manganese-bearing sequences, with the solubilization of their components, is

greater in the rainy season, with the leached manganese, and iron, being transported in the form of gelatinous acid compounds. Accompanying a change of pH, a loss of water, the action of bacteria, or other causes, the compounds are deposited on the walls of fractures of the rocks being weathered or on larger open surfaces. Over time, the rocks are replaced and, in the open spaces, mammillary and columnar structures are formed (Valarelli, 1967).

Cryptomelane (KMn_8O_{16}) is the main ore mineral of the deposit. It crystallizes in the form of dust or fine fibers less than 0.5 millimeter in diameter, which are difficult to see with a hand lens. They coalesce into compact masses, and can only be identified with X-ray methods (Marvin 1956, Gault 1959, Castro 1963, Valarelli 1966, 1967). Chemical analysis of four selected samples of massive cryptomelane showed that manganese oxides constituted more than 90% of the mineral, followed by silica (0.2 to 1.5%), and oxides of potassium (1 to 2%), aluminum (1 to 6%), sodium (0.2 to 0.7%), and iron (0.2 to 0.3%), in addition to smaller quantities of other oxides (Valarelli 1967).

Among other minerals, lithiophorite [$Li(Al,Fe)MnO_3*H_2O$], which is similar to cryptomelane, was identified in some samples (Marvin 1956, Castro 1963), mainly in those of gondites (Valarelli 1967). Crystals of pyrolusite (β-MnO_2) pseudomorph after manganite (Valarelli 1966, 1967), were observed in cavities.

The massive ore was formed by the total or partial replacement of the queluzites and gondites by oxides and hydroxides of the solubilized manganese, iron, silica, and aluminum. Dissolution and reprecipitation of these components continued to occur along zones of fractures and in areas with remaining silicates, leading to the formation of cavities (Fig. 2A), which have bottom and walls covered with cryptomelane with botryoidal or mammillary textures, and with pyrolusite crystals on their surfaces (Fig. 2C, D, E). The process leads to a continuous increase in the manganese grade (Nagell 1962).

At deeper levels, the leached compounds move away from the source rock, impregnating adjacent country rocks. In the soil profile near the deposit, manganese and iron appear as concretions. In this case, it seems that the elements moved laterally and, in dry seasons, they also moved upwards from the water table, precipitating around quartz or aggregates of clays, forming concretions. When they occur together in the same area, the concretions richer in manganese are seen below those richer in iron.

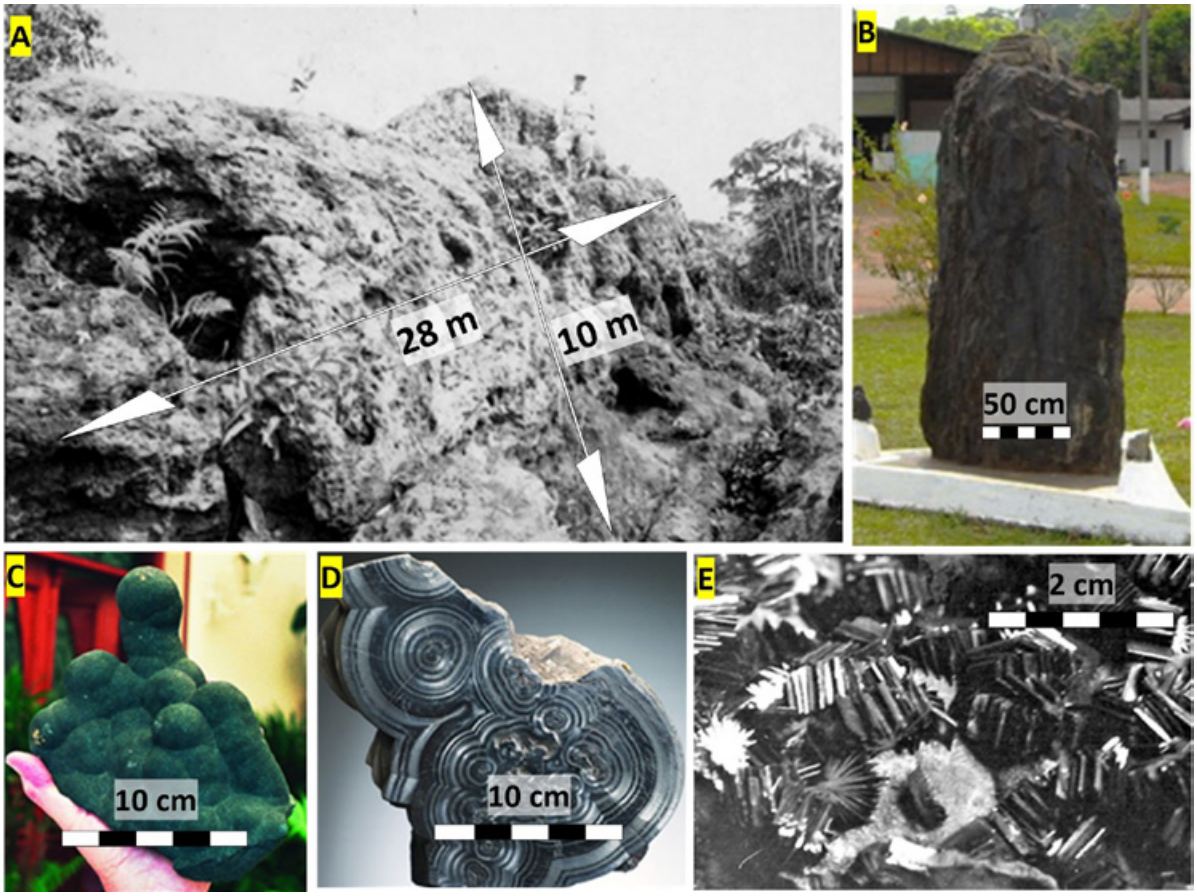

FIGURE 2. Images of the manganese oxide ore. (A) Photo taken at the time of discovery of the T-20 mine: a 10-meter high ridge of massive ore. The geologist in the photo is used as a size reference. There are large dissolution caves, and indications of layering with a dip to the left (northeast). (B) Block of the massive ore, exposed as a monument, at the center plaza of the town of Serra do Navio. A subvertical layering might be seen in the block. (C) Mammillary cryptomelane, deposited in a solution cavity of the ore. (D) Section of one of such structures, showing the group of coalescent columns of the mineral. (D) Pyrolusite crystals, showing rosette structure, in an ore cavity. Note the white crystals of gibbsite at the lower center. Photos A, B and E obtained from the author's files. Photos C and D were copied from "Minerais e Pedras Preciosas do Brasil, Solaris Edições Culturais, 2010", with authorization of the authors, Carlos Cornejo and Andrea Bartorelli.

1.6. Mining and ore beneficiation of the manganese oxide ores

Mining was done open cast, with the overburden of the ore deposited on the flanks of the hills. During the life of the mine, the run-of-mine was composed of mixtures of ores from different types and areas, of high and medium grades. The proportions of the various ore types in the mixture were programmed to reach the grade desired by the market, without reducing the life of the mine. Most of the resources of low grade (below 30-32% Mn), those which were not included in the run of mine, were stockpiled in the mine areas.

As described above, the feed to the plant was made of high-grade ores, together with variable percentages of weathered gondites and schistose ores. After crushing, it was submitted to a sequence of washing and screening processes, to remove, as tailings, the fine-grained fragments of the gangue, and the very fine-grained manganese hydroxides which are not recoverable in the process. The losses of manganese represented less than 5% of the metal contained in the feed to the plant. In recent years, ores from low-grade areas of the mines were also sent to the plant, and, after crushing and washing, were submitted to density separation, recovering the heavier fragments, as commercial products, and discarding the lighter ones, as tailings of very low grades (Rodrigues et al. 1986).

After these phases, the denser, clean and screened fragments, constituting about 90% of the tonnage supplied to the plant, were classified according to the grade and size of their particles, and sent to the port for shipment (Rodrigues et al. 1986; Costa 1997).

2. Regional geology

2.1. The basement and the Vila Nova greenstone belt

The Precambrian Shield of Amapá is part of the Maroni-Itacaiunas tectonic province (Tassinari et al. 2004; Rosa-Costa et al. 2006, Barreto et al. 2013, Rosa-Costa et al. 2014), which is formed by an Archean basement made of gneisses, migmatites, granitic intrusives, and granulites, locally covered by fold belts of greenstones of the Paleoproterozoic Vila Nova Group (Fig. 1) (Lima et al. 1976). All of these rocks are metamorphosed into the amphibolite facies, and intruded by granitic rocks. In two small areas, one in the mid-course of the Jari River, and the other extending from the mid-course of the Falsino River (Scarpelli 1969) to near Tartarugal, the lithologies of the basement and of the Vila Nova Group were metamorphosed to the granulite facies (Scarpelli 1966, João et al. 1979, Scarpelli and Horikava 2018).

2.2. The Jornal Formation, base of the Vila Nova Group

The fold belts of the Vila Nova Group, which occur all over the Amapá and the eastern part of most of the northern part of Pará, present, at the base, a unit of orthoamphibolites, which are the product of metamorphism of mafic and minor ultramafic volcanic rocks (Dardenne and Schobbenhaus 2001, Barreto et al. 2013; Hoffmann et al. 2018). The same setting is seen across the Itacaiunas-Maroni tectonic province, with the orthoamphibolites named Paramaca, in French Guiana, Paramaka, in Suriname, Tenapu, in Guyana (Gibbs and Barron 1993), and El Callao, in Venezuela (Bellizia 1972, Pasquali 1972). Gondites were seen in metasediments associated with some of these belts in French Guiana, Suriname, Guyana and Venezuela; some of them associated with carbonaceous schists (Choubert 1973).

In Brazil, these orthoamphibolites are known as the Jornal Formation (Nagell 1962, Scarpelli and Horikava 2017). In Serra do Navio, the amphibolites show few and narrow intercalations of micaceous quartz schists, and reaches more than 3 kilometers in thickness (Scarpelli and Horikava 2017), dipping to the northeast.

2.3. The sedimentary sequence of the greenstone belts

In the central zone of Amapá and northwest of Pará, the Vila Nova Group presents a column of metasediments covering the Jornal Formation. They were deposited in a former basin that extended for, at least, 700 kilometers from east to west and 90 kilometers from north to south (Scarpelli and Horikava 2018).

These sediments are typical of shallow coastal environments, with alternations of clastic and chemical units, well developed planar bedding, fine-grain size, and, with a few exceptions, good gradual transition zones between the lithologies. Calcic marbles and manganese-rich queluzites occur in the basal Serra do Navio Formation, whereas calcic to dolomitic marbles, and oxide iron formation, occur in the overlaying Serra da Canga Formation (Scarpelli and Horikava 2017).

The metasediments are folded, with the fold axis striking northwest, and, on the surface, following elongated ridges and plateaus that reach up to 200 to 250 meters above the countryside. Due to the rainy weather, the metamorphic foliation and their fine-grain size, they weather easily, with the alteration reaching 60 to 100 meters below the hill tops. In consequence, outcrops are scarce, represented by lithologies more resistant to erosion, such as a few quartzites, iron formations and oxidized manganiferous layers. The flat surface of the plateaus is usually covered by a lateritic duricrust of several meters in thickness.

2.4. The manganiferous Serra do Navio Formation

The Serra do Navio Formation concordantly overlays the Jornal Formation and dips to the northeast (Fig. 3). Outcrops of the formation are scarce, and the unit was defined based only on geologic sections made with core drilling and geological maps of the mines. Until now, the formation was only reported in Serra do Navio, and no place else, but obviously this may change as studies and drilling are carried out in other portions of the sedimentary basin. The regional exploration work has indicated that the formation extends northwestwards for at least 16 kilometers, with the manganese ore deposits observed in the central 10 kilometers of that extension. Due to the folding and the lack of outcrop, the thickness of the formation is not known and is assumed to be of less than 500 meters.

The Serra do Navio Formation is covered in the east by the Serra da Canga Formation, which constitutes the upper portions of the highest topographic ridge of Serra do Navio (Fig. 3). Further to the east, the two formations are cut by the intrusive Amapari granite (Scarpelli and Horikava 2017).

From the southeast to the northwest, the manganese deposits or mines were named T-11, T-6, T-4, T-20, A-3, A-12, C-4, C-5, C-2, C-01, and F-12. No mineralization was found

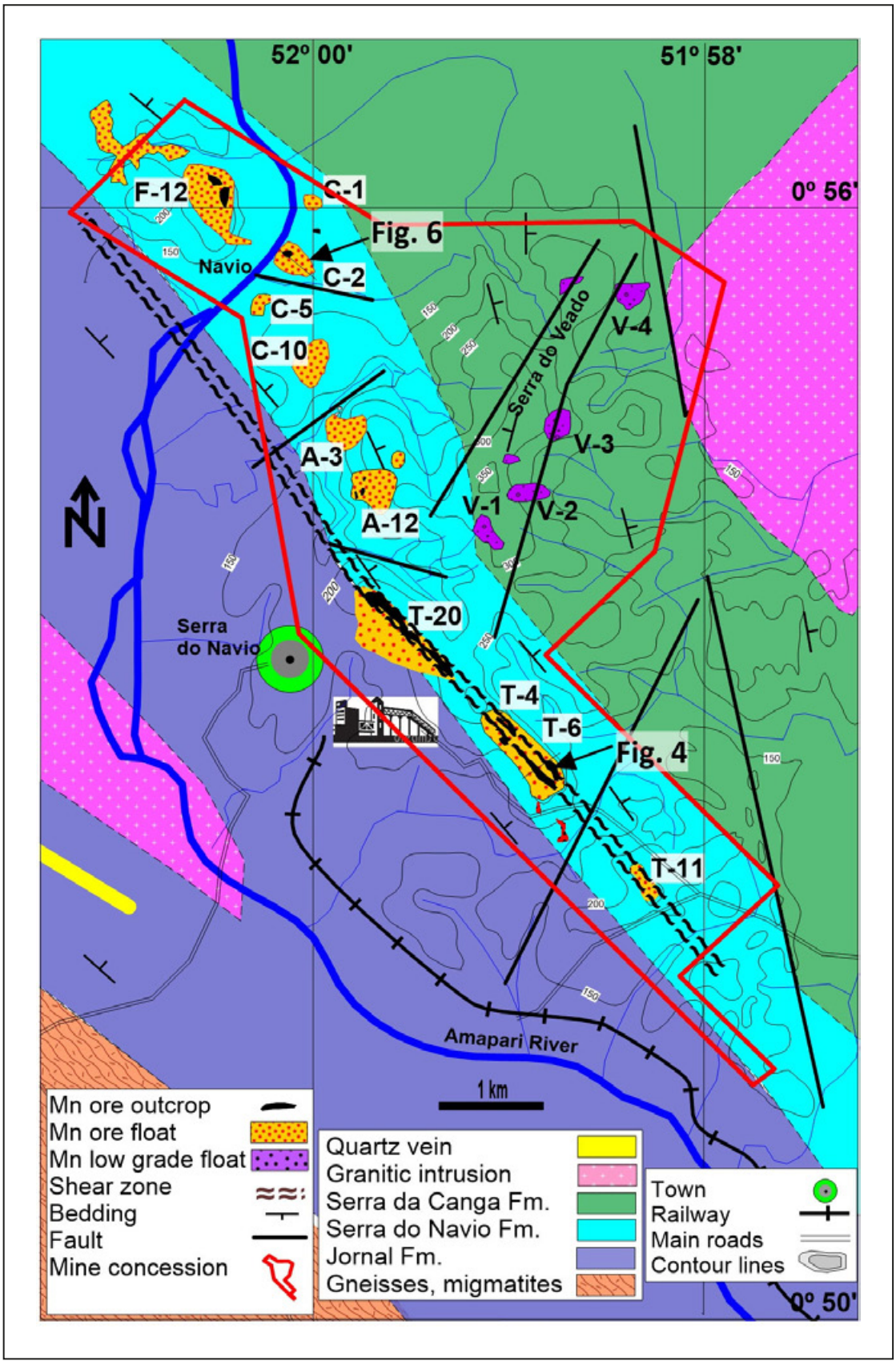

FIGURE 3. Geological map of Serra do Navio. The masses of supergene manganese oxide ores outcrop atop the ridges with the Serra do Navio Formation, which dips to the northeast. The formation covers the Jornal Formation, and is overlain by the Serra da Canga Formation. The Amapari granite intrusion crop-out to the east. An extensive shear zone follows the line of mines T-11, T-6, T-4 and T-20. Northwards of T-20, the line of deposits is at the east of the shear, with deposits A-12, A-3, C-10, and C-5. Stratigraphically above, there are the deposits C-2 and F-12. The Serra da Canga Formation has occurrences of low-grade gondite ores. (Figure based on Scarpelli and Horikava 2017).

to the southeast of the T-11 and to the northwest of the F-12, although the formation continues for a few kilometers in these directions.

The geology of the area and of the ores was first described by Nagell (1962). The first intersection of the queluzites protores was observed in one of the first holes at the T-6 mine (Fig. 4), 50 meters above the contact with the Jornal Formation (Nagell and Silva 1960, Silva et al. 1963; Scarpelli and Horikava 2017). This drill interception was made where today is the Poço Azul, a tourist attraction of Serra do Navio.

A prominent shear striking northwest and dipping to the northeast, parallel to the foliation of the rocks, follows the Serra do Navio Formation for 4.5 kilometers, along the line marked by the T-11, T-6 / T-4 and T-20 mines, continuing northwards through the Jornal Formation. Where it crosses the Amapari River (Fig. 3), a 100-meters-wide zone of the Jornal orthoamphibolites appears recrystallized to chlorite schist. The shear shows a left-lateral displacement, coupled with the up-thrown of the northeastern side over the southwestern.

Tonnage-wise, the greatest orebodies of the district, with thickness ranging from 20 to 50 meters, were found in the T-6 / T-4 and T-20 mines, in the footwall of the shear. They dip 70º to the northeast.

Above them, there are other masses of mineralization, which are stratigraphically within the wide shear zone and were pushed upwards and folded into synclines and anticlines (Fig. 4). In this tectonic zone, the intervening schists locally have structures similar to those of plastic folding (Fig. 5). These isolated masses of ore are considered to be part of other lenses of weathered queluzite, pushed upwards along the shear zone.

The observation of the extension of the orebodies in these mines offers a quantification of their lenticular shape. The southern one, the T-11, is the thinnest and has 600 meters in length. After a barren gap of 800 meters, appear the T-6, with 500 meters in length, and, after 200 meters, the T-4, with 300 meters. To the north, after a gap of 400 meters, there is the T-20, with 1,500 meters in length. So, over the extension of 4,300 meters, there are four orebodies totaling 2,900 meters of mineralization. In these mines, the orebodies above the shear zone are shorter, due to the faulting, varying from 200 to 400 meters in length.

The mines A-3, C-10, C-2 and F-12 are located outside the shear zone and more distant from the Jornal Formation. In these mines, the formation appears as simple folds, with gentle angles of dip of the main foliation to the northeast and a low angle of dip of the fold axis to the northwest.

A program of short spaced holes drilled at the C-2 mine revealed that the host lithologies constitute a metamorphosed megacyclothem, with the queluzites occurring near the top of each cycle (Fig. 6). The drilling of this mine revealed three complete cyclothems, and the formation was still open at depth.

Overall, it is not known how many cyclothems exist in the Serra do Navio Formation. It is accepted that those of the C2 mine constitute the upper three, and those of the T-6 / T-4 and T-20 mines constitute the lower two. There are petrographic and structural similarities between the deposits of T-6, T-4, T-20, A-12, A-3, C-10, and C-5, and all of them appear near the contact with the Jornal Formation. On the other hand,

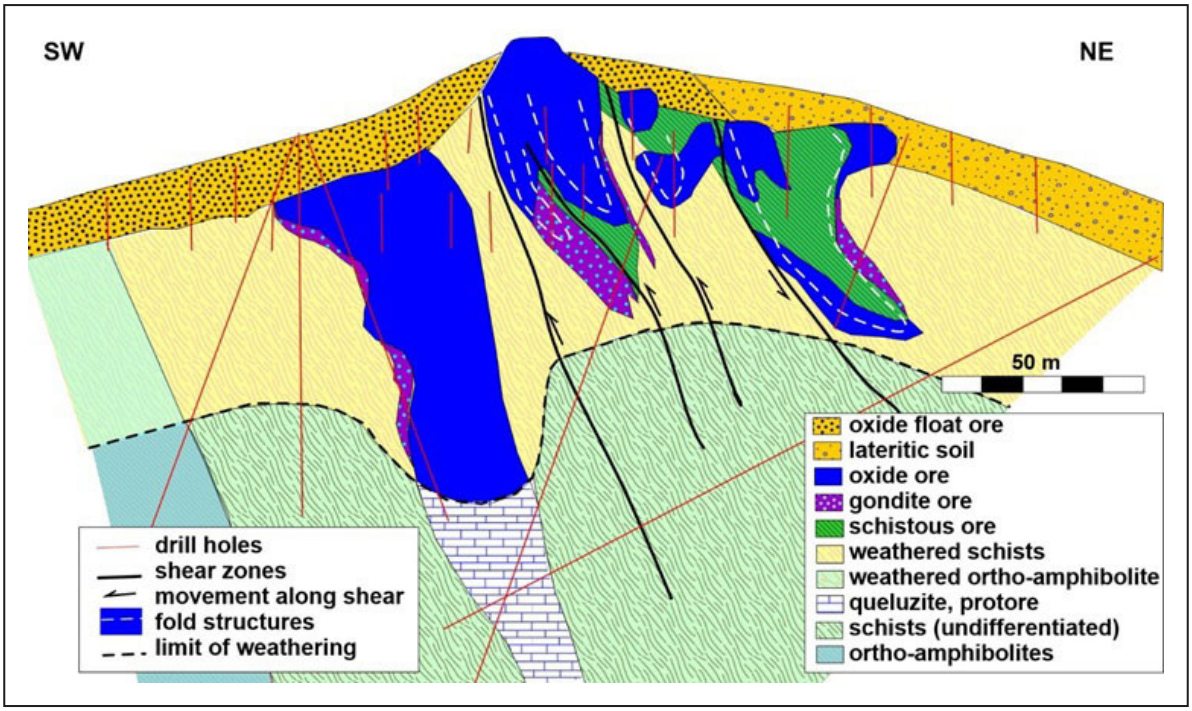

FIGURE 4. Cross section of the T-6 mine. The orebody at the left of the section, with more than 20 meters of thickness, occurred between the shear zone, at the right, and the orthoamphibolites of the Jornal Formation, at the left. It replaces the queluzite until about 100 meters below the surface, with the queluzite extending in depth. To the right, smaller masses of other ore lenses were uplifted along faults related to the transcurrent shear zone, creating complex geological structures. These main blocks of ore are derived from queluzites and gondites. Adjacent masses of schists are partially impregnated with or replaced by with manganese oxides, constituting the schistose ore. On the western slope of the ridge, there is a cover of float ore, with boulders of massive and high-grade manganese oxides. Similar structures occur at the T-4 and T-20 mines. (Figure reproduced from Scarpelli and Horikava 2017).

FIGURE 5. At the T-20 mine, and in the shear zone, view of a highly deformed quartz-biotite schist, of the biotitic facies. The photo faces southeast, and the drag folds indicate that the rocks were uplifted from the northeast. The fold axis has a small angle of plunge, to the north-northwest.

there are also similarities between the deposits C-2, C-1 and F-12, which are located face-to-face, at the margins of the Amapari River, and at a higher stratigraphic elevation. These observations indicate that at least five cyclothems might exist.

2.5. The sedimentary facies of the Serra do Navio Formation

The formation is a metamorphosed megacyclothem, that is, a metamorphosed column of metasediments deposited in superposed and similar cycles of sedimentation (cyclothems), in a near-shore marine and littoral environment affected by a fluctuating sea level (Fig. 7). Each of the cyclothems is made of three metamorphosed sedimentary facies, the quartzose, the biotitic and the graphitic. Whereas the lower facies, the quartzose, is a product of an oxidizing open sea coastal environment of deposition, the upper facies, the graphitic, is characteristic of an environment of reduction, with restrict circulation, lagunar and possibly swampy (Scarpelli 1966, Scarpelli 1973). The two facies contain important layers of carbonatic rocks, calcium-rich in the quartzose facies and manganese-rich in the graphitic facies. The two facies are separated by the intermediate biotitic facies. The mineral composition of the metamorphosed clastic units of the formation is shown in Table 1. They are about the same for all lithologies, with some variation in the percentages. The composition of the minerals that constitute the carbonatic units is shown in Table 2. In this case, the differences in composition are large.

A characteristic of these cyclothems is a transitional contact between the three facies, in contrast with the

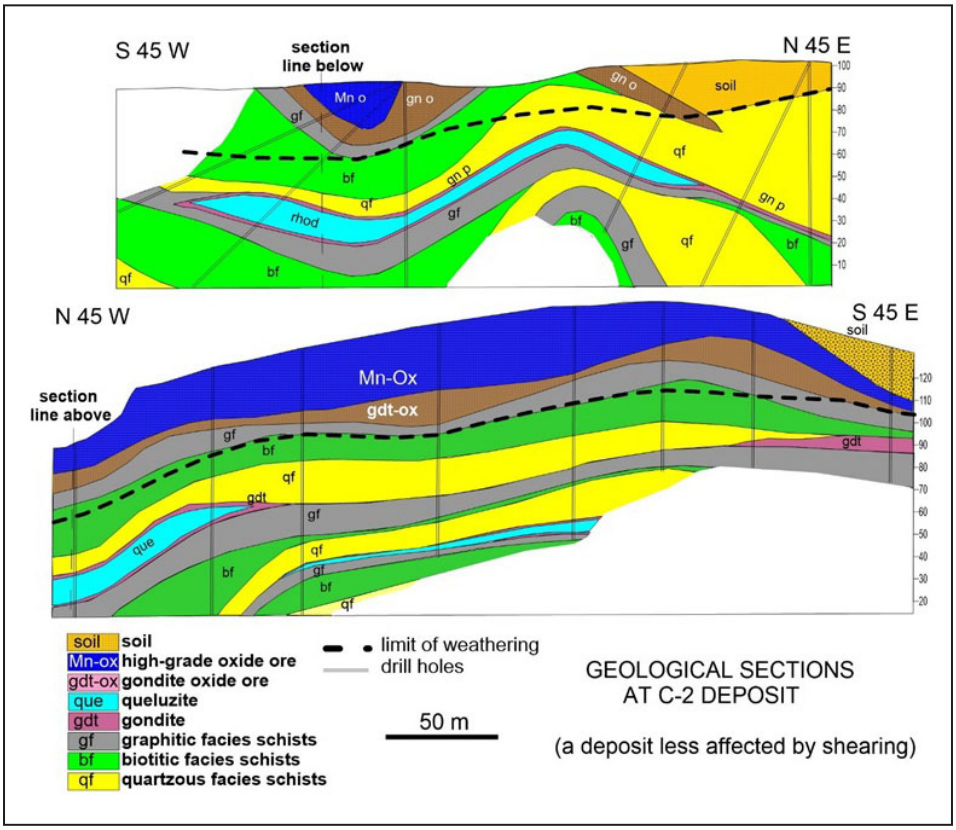

FIGURE 6. Cyclothems of the Serra do Navio Formation in the C-2 mine. The section above is perpendicular, and that below is parallel to the fold axis. Three cycles of deposition are shown, with the upper cycle being the thicker and presenting the larger volume of ore (Scarpelli 1973).

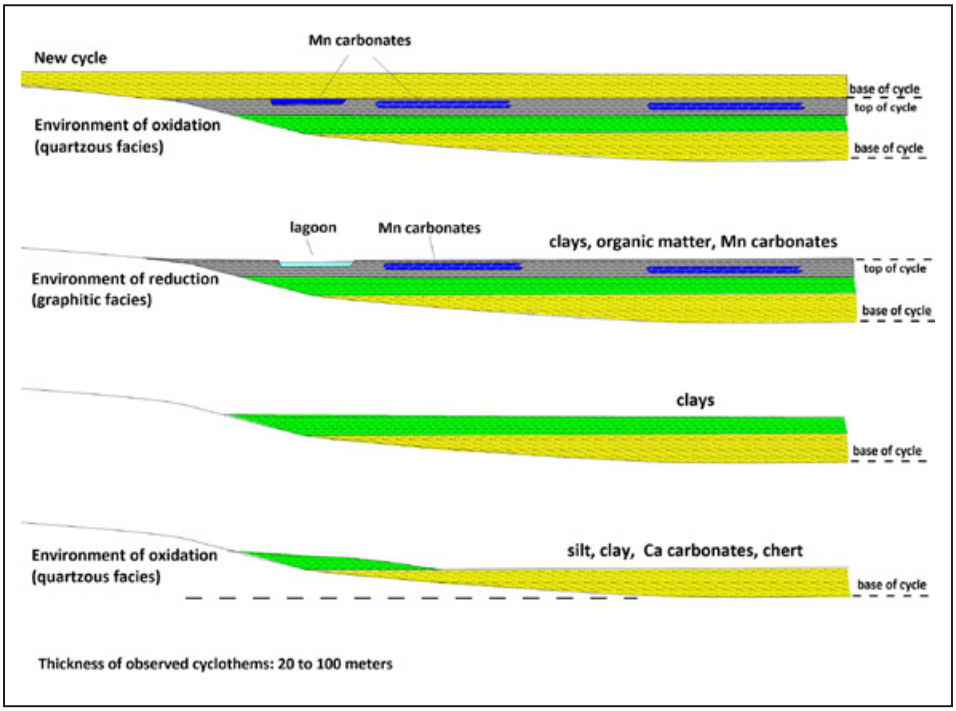

FIGURE 7. Sequence of deposition of the sediments that constitute the megacyclothem of the Serra do Navio Formation. The lower unit of each cycle, deposited in open sea environment, consists of alternating layers of siltstones, clays, limestones and chert. It grades to an intermediate coastal clayey sequence, which passed upwards to a clayey sequence with organic matter, deposited under restricted water circulation. Lagoons appeared at the upper part of these sediments, and became site for deposition of manganese carbonates, together with some clays and chert. The contact with the overlying open sea sediments of the next cycle is always abrupt.

TABLE 1 - Mineral composition of the non-carbonatic units of the Serra do Navio Formation.

Facies	Quartzose Facies			Biotitic Facies			Graphitic Facies		
Samples	(16 samples)			(13 samples)			(14 samples)		
Measurement	Average	Max-Min	Presence	Average	Max-Min	Presence	Average	Max-Min	Presence
	%	%	%	%	%	%	%	%	%
quartz	30	60-3	100	29	50-20	100	24	38-8	100
biotite	9	33-0	63	34	53-20	100	12	34-0	93
graphite	4	9-0	75	4	8-tr	100	26	45-15	100
muscovite	8	25-0	75	3	8-0	77	4	13-0	57
plagioclase	12	34-0	56	4	25-0	38	3	25-0	29
sillimanite	3	35-0	31	8	25-0	77	2	5-0	57
andalusite	4	17-0	31	4	26-0	46	7	20-0	57
staurolite	tr	tr-0	6	tr	1-0	38	5	10-0	71
garnet	5	35-0	94	8	25-0	85	6	10-0	71
cordierite	-	-	-	2	18-0	15	-	-	-
tremolite	10	50-0	50	-	-	-	-	-	-
diopside	1	10-0	13	-	-	-	-	-	-
titanite	1	6-0	38	-	-	-	tr	1-0	7
calcite	1	7-0	13	-	-	-	tr	1-0	7
hornblende	3	8-0	19	-	-	-	-	-	-
tourmaline	3	20-0	75	1	3-0	92	2	6-0	71
sulfides (*)	2	6-0	63	1	3-0	69	1	2-0	71
epidote	3	15-0	31	1	5-0	8	4	30-0	29
chlorite	1	5-0	38	1	5-0	31	4	45-0	21
TOTAL	100			100			100		

The presence of the minerals was obtained by continuous readings along 8 lines crossing the sections
Column 'average"' refers to the average occupied by the minerals in the examined thin sections.
Column 'Max-Min' refers to the maximum and minimum areas occupied by the mineral in the examined thin sections
Column 'Presence' indicate the percentage of the thin sections that present the mineral
Sulfides: Pyrite is common, followed by pyrrhotite, next by chalcopyrite, and rarely by arsenopyrite.

TABLE 2 - Mineralogy of marbles and calc-silicate rocks of the Serra do Navio Formation.

Lithology	Marbles		Calc-silicate rock	
samples	2		6	
Measurement	Average	Max-Min	Average	Max-Min
	%	%	%	%
calcite	93	95-90	10	15-04
diopside	4	8-00	65	75-35
tremolite	-	-	6	15 - tr
grossularite	-	-	9	15-01
chlorite	1	2-00	5	30-00
biotite	1	2-00	-	-
titanite	-	-	2	9 - tr
pyrrhotite	-	-	2	3-02
graphite	-	-	tr	tr
Total	99		99	

The presence of the minerals was obtained by continuous readings along 8 lines crossing the sections
Column 'average"' refers to the average occupied by the minerals in the examined thin sections.
Column 'Max-Min' refers to the maximum and minimum areas occupied by the mineral in the examined thin sections

abrupt contacts between the individual cyclothems (Fig. 8). Occasionally, minor sharp contacts were seen within the cyclothems, reflecting tectonic disruptions caused by faults or by transpositions on the planes of foliation during folding. These disturbances are usually identified based on features of the structure of the rocks.

The lower facies of each cyclothem, the quartzose, is of a light gray to pale yellowish color and is made of alternating bands of metachert, fine-grained muscovite quartzites, fine to medium-grained almandine garnet-biotite-quartz schists, calcite marbles, and lenses of calc-silicate rocks containing diopside, grossularite, tremolite, and calcite (Fig. 9). These rocks are the product of metamorphism of a sequence of layers of chert, siltstones, pelites and calcium-carbonates, which show clear planar bedding, outlined by differences in mineral composition of the individual beds. Quartz-feldspar metasiltstones are mostly composed of quartz, plagioclase (bytownite), titanite, muscovite, and porphyroblasts of almandine. Some of these porphyroblasts grew laterally, replacing favorable horizons. Layers originating from chert are marked by the predominance of quartz and less plagioclase. and, usually have some tremolite. The thickness of the layers of calcite marbles, which usually contain tremolite and diopside porphyroblasts, varies from centimeters to tens of meters. Calc-silicate layers, marked by larger crystals of diopside or aggregates of tremolite, characterize the original limestones mixed with chert of silt. Sulfides, mostly pyrrhotite and pyrite, and occasional chalcopyrite, are minor constituents of the rocks of this facies.

FIGURE 8. This photo taken in 1968, at the northern end of mine A-12, shows a contact of the graphitic schist (at the lower right-hand side) that constitute the upper portion of the lower cyclothem of the A-12 mine, with the quartz-bearing schist, (at the upper left-hand side), which constitutes the base of the second cyclothem of the area. Rains and erosion already destroyed the exposure.

The quartzose facies is covered by the biotitic facies, which is a metamorphosed metapelite with light to dark-brown color. It appears as an almandine garnet-quartz/plagioclase-biotite schist, (Fig. 10) occasionally with muscovite. It is medium-grained, with a strong schistosity and weak layering. Bedding becomes visible where there are bands richer in quartz and feldspars. Biotite often appears elongated parallel to the fold axis. Porphyroblasts of almandine are very common, occasionally with poikilitic quartz and inclusions. This unit presents staurolite, andalusite, cordierite, and sillimanite, suggesting that the rock has reacted to distinct conditions of regional metamorphism. Pyrite is a common minor constituent of the rock, not rarely accompanied by chalcopyrite.

The upper facies is graphitic, represented by a black and fine-grained biotite-quartz-graphite schist (Fig. 11), the product of metamorphism of a metapelite rich in organic material (Scarpelli 1966, Scarpelli 1973). Bedding is recognizable where there is more quartz or graphite. The unit presents accessory fine grains of pyrite and chalcopyrite, with occasional arsenopyrite. Scarpelli (1966) considered two alternatives for the origin of the graphite: directly from organic material or from some form of liberation of carbon of carbonates. The complete absence of graphite in the layers of limestone of the quartzose facies, which occur above and below the graphite facies, discards the carbonates as a source. In addition, whereas the deposition of manganese carbonates and organic material requires a reducing environment, the deposition of limestones requires an oxidizing environment.

2.6. The queluzites

Lenses of queluzites occur at the upper part of the graphite schists, often covered by a narrow zone of graphite schist, below the sharp contact with the metasediments of the quartzose facies of the cyclothem above. These lenses have a thickness of a few to near 50 meters and vary in length from a few hundred meters to 1.4 kilometers, as seen at the T-20 mine.

At the upper and lower contacts of the queluzites with the graphite schist, there is a transition zone consisting of gondites (Fig. 12), presenting spessartite, quartz, graphite, and a manganiferous amphibole identified as richterite (Valarelli 1967), and no carbonate (Table 3). Their garnets have diameters of 2 to about 5 millimeters, frequently with growth banding and indications of rotation during growth.

The queluzites are essentially made of rhodochrosite and spessartite (Fig. 13, and Table 3), with the carbonate showing several phases of crystallization due to several tectonic events. Spessartite typically has a light-gray color and is smaller than

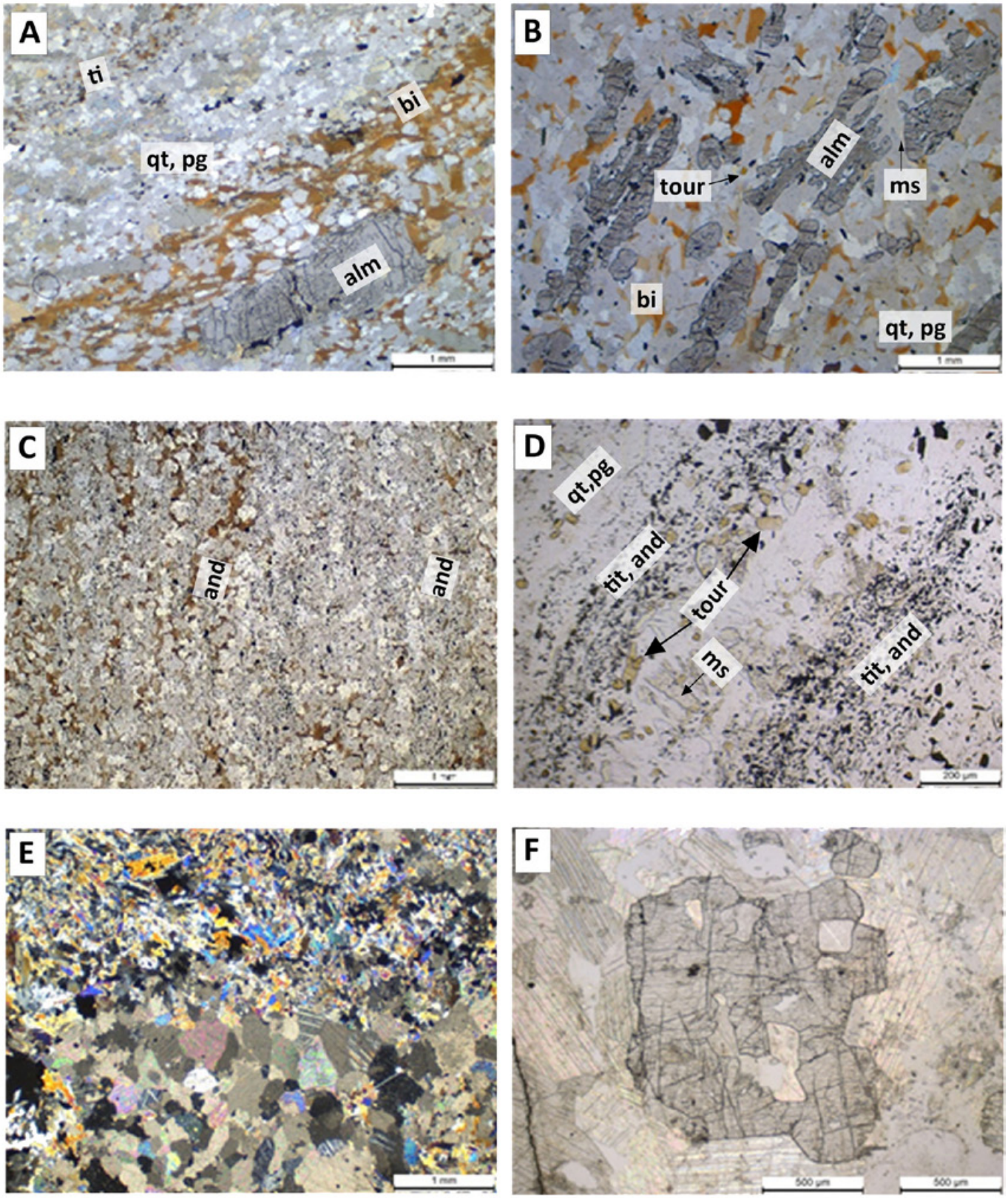

FIGURE 9. Views of the quartzose facies exposing the primary layering. (A) From mine T-4, a well layered almandine-biotite-quartz-plagioclase schist, with the almandine elongated parallel to the layering, following favorable conditions. Above, a parallel line of titanite also marks the layering. (B) From mine C-2, a similar lithology, with muscovite and scattered tourmaline, and with a prominent elongation of almandine parallel to the layering. (C) From mine T-4, layering marked by a higher concentration of biotite on the left, and with andalusite on the right. (D) From mine C-2, a well layered muscovite-oligoclase-quartz schist, with some layers containing fine-grained titanite and andalusite. In the center, a layer with muscovite and tourmaline. The muscovite is oriented perpendicular to the layering. (E) From mine C-2, a contact between a tremolite-rich layer, above, and a calcite-marble, below. (F) From mine C-1, a calcite marble with a euhedral porphyroblast of diopside containing inclusions of calcite.

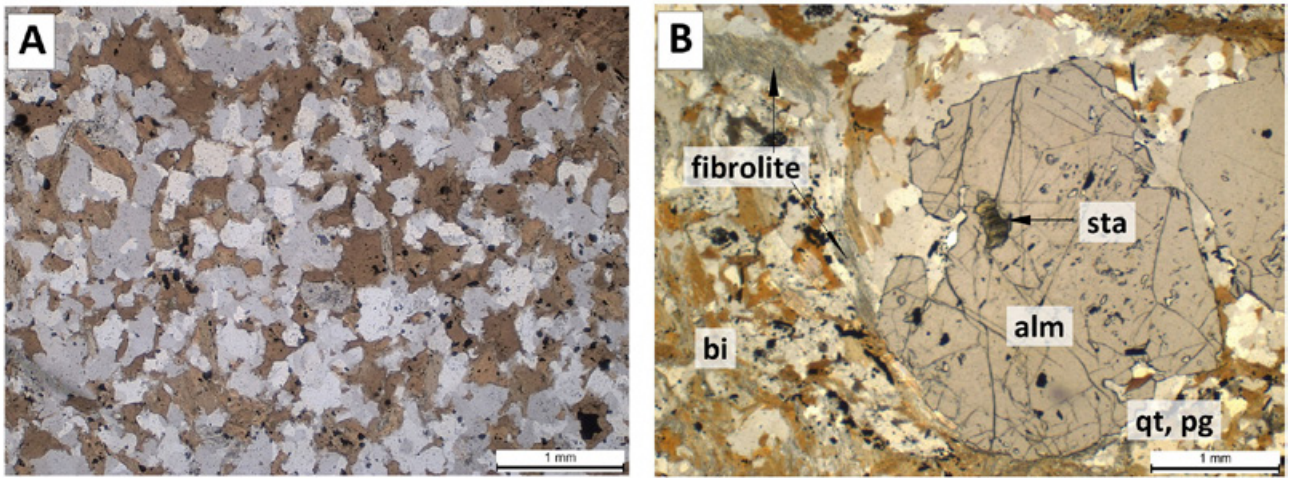

FIGURE 10. (A and B) Biotite schists of the biotitic facies. Biotite and quartz predominate over plagioclase, together with dispersed coarse-grained pink almandine garnets. In (B), an inclusion of staurolite in the almandine, and, to the left of it, bundles of fibrolite marking a zone of displacement along the foliation. Most of the opaques are pyrite.

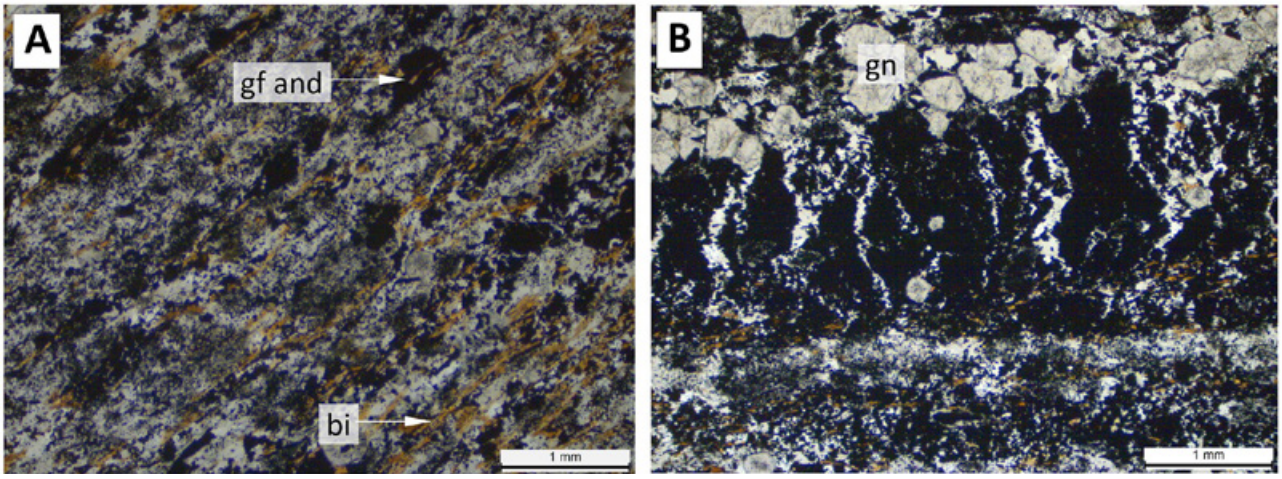

FIGURE 11. Well layered graphitic facies rock, from the T-6 mine. (A) Graphite occurs as inclusions in andalusite and dispersed along the bands of quartz, plagioclase, and biotite. (B) A massive layer of graphite and pyrite is fractured by shrinkage, with the fractures filled with quartz. Above, it is flanked by a layer with spessartite, and, below, by bands of quartz.

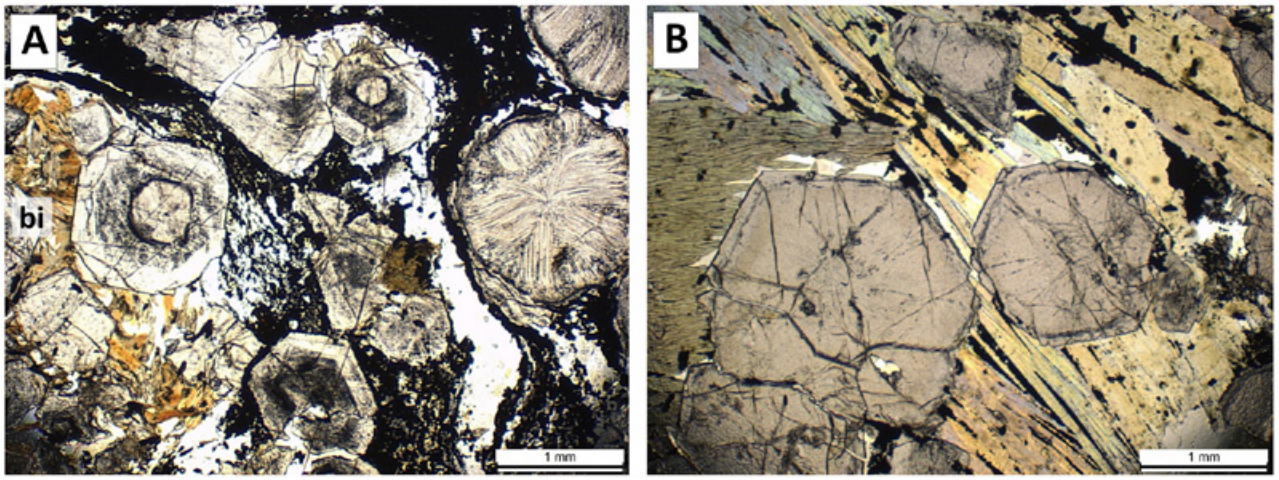

FIGURE 12. Images of gondites. (A) From mine C-1, porphyroblasts of spessartite in a mass of graphite, quartz and biotite. The garnets show phases of regrowth and indications of rotation during growth. (B) From mine T-20, the garnets are larger and accompanied by an amphibole, possibly richterite.

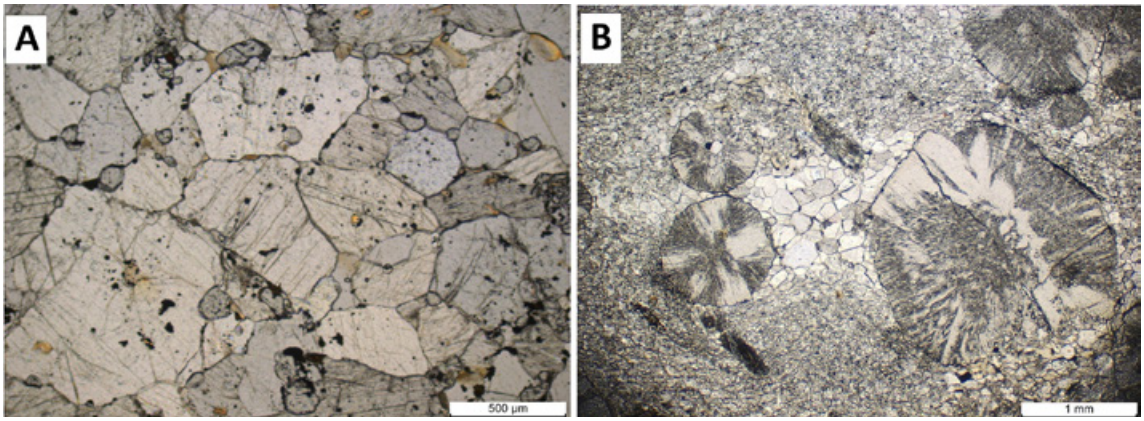

FIGURE 13. Images of queluzites. (A) From mine A-12, rhodochrosite, with a mosaic texture, constitutes more than 85% of the sample. It is accompanied by some spessartite, rhodonite, and graphite. (B) From mine T-6, rhodochrosite presents a mosaic texture only in the zone of pressure shadow between crystals of spessartite. Outside this area, it was tectonically ground to a fine-grain size.

2 millimeters in diameter. Dispersed, or following some of the layers of rock, the queluzites also contain (Fig. 14) pinkish porphyroblasts of rhodonite and grey picrotephroite (optically identified by Scarpelli 1961, based on tables of Winchell and Winchell 1959), usually followed by the amphibole richterite (Vallarelli 1967). Rhodonite and picrotephroite often occur close by, and not rarely cross each other. They possibly originate from the reaction of carbonates with silica, or silicates, during a thermal episode. At the F-12 mine, they are concentrated in a few lenses concordant with the bedding. As for accessories, the queluzites present graphite, orthoclase, and very minute grains of sphalerite (formerly described as piedmontite), gersdorffite and niccolite (Scarpelli 1973, Chisonga et al. 2012).

Table 3 shows two estimates of the mineral composition of the queluzites and gondites, one with an actual

TABLE 3 - Mineralogy of gondites and queluzites of the Serra do Navio Formation.

(From Scarpelli W. 1966)								(From Chisonga, B.C. 2012)	
	Gondites		**Queluzites**					**Queluzites**	
Mine	**diverse areas**		**T-4 / T-6 / T-20**		**C-1 / C-2**			**F-12**	
Samples	**8**		**7**		**12**			**18 core samples**	
Measurement	**Average**	**Max-Min**	**Average**	**Max-Min**	**Average**	**Max-Min**		**Estimation of presence**	**Estimation of dominance**
	%	**%**	**%**	**%**	**%**	**%**			
rhodochrosite	5	27-00	75	99-50	30	75-02		major - absent	1.1
spessartite	65	80-60	8	20-04	13	35-05		major - trace	1.7
picrotephroite	-	-	0.5	3-00	40	70-15		major - absent	1.9
rhodonite	2	6-00	7	40-00	10	40-00		major - trace	2.2
Mn-amphibol	8	25-00	1	4-00	tr	tr-00		minor - absent	0.9
biotite	2	10-00	0.5	2-00	1	0-04		minor - absent	1.9
graphite	5	10-03	6	25 - tr	6	15-02			
zoisite	tr	tr-00	tr	tr-00	tr	2-00			
sphalerite	tr	tr - tr	tr	tr - tr	tr	2 - tr			
other sulfides (*)	-	-	tr	tr - tr	tr	1 - tr			
pyrrhotite	1	3-00	-	-	-	-			
quartz	9	10-03	-	-	-	-		minor - absent	0.7
titanite	3	10-00	-	-	-	-			
TOTAL	100		97		100				

From Scarpelli, 1966:
The presence of the minerals was obtained by continuous readings along 8 lines crossing the sections
Column 'average"' refers to the average occupied by the minerals in the examined thin sections.
Column 'Max-Min' refers to the maximum and minimum areas occupied by the mineral in the examined thin sections
Other sulfides: In all samples of queluzites: niccolite, and gersdorffite. In a few samples: cubanite.

TABLE 4 - Chemical analysis of gondites and queluzites.

Elements	ICOMI ASSAYS									CHISONGA ASSAYS from F-12		
	Gondite	Transition		Queluzites						Mn-silicate	Mn-calcite	Rhodochrosite
%	T-6	T-6	T-6	T-6	T-6	T-6	C-2	C-2	T-20	rock	marble	marble
Mn	3.6	27.7	24.1	36.6	35.7	33.7	31.8	29.0	33.0	28.6	38.3	39.1
SiO_2	49.7	32.6	34.7	6.6	15.3	17.1	3.5	19.0	11.0	39.7	23.8	5.2
CO_2	1.2	19.3	8.6	33.4	27.5	26.3	32.4	n.a.	33.0	<4.9	<5.8	<27.0
Fe	4.8	2.8	3.6	1.3	3.7	3.7	0.4	4.0	3.0	4.1	3.7	1.4
Al_2O_3	12.7	3.6	8.9	2.9	1.9	2.4	2.6	6.0	7.0	3.7	2.9	2.6
C	3.4	8.2	4.3	n.a.	7.9	9.3	n.a	n.a.	n.a.	n.a.	n.a.	n.a.
CaO	3.5	0.8	1.7	4.9	0.6	0.7	8.1	n.a.	3.0	4.4	5.3	6.9
MgO	3.1	0.2	1.7	2.9	0.4	0.3	3.7	n.a.	5.0	3.1	5.8	4.2
Na_2O	<0.05	<0.05	<0.05	n.a.	<0.05	<0.05	0.3	n.a.	n.a.	<0.1	<0.1	<0.1
K_2O	<0.05	<0.05	<0.05	n.a.	<0.05	<0.05	0.1	n.a.	n.a.	<0.2	0.3	0.1
S	1.0	0.1	0.6	n.a.	0.01	0.3	1.0	n.a.	n.a.	n.a.	n.a.	n.a.
As	<0.1	0.2	0.1	n.a.	0.2	0.1	n.a.	n.a.	n.a.	n.a.	n.a.	n.a.
P	0.08	0.03	0.03	n.a.	.04	0.04	n.a.	n.a.	n.a.	n.a.	n.a.	n.a.
Total	84.0	95.6	88.5	88.6	93.4	93.9	83.9	58.0	95.0	88.5	85.9	86.4

n.a.: not assayed
Analysis from ICOMI (Scarpelli W. 1966, and 1973)
Analysis from Chisonga (Chisonga B.C. et al. 2012)

measurement of the areas occupied by the minerals in thin sections (Scarpelli 1966, 1973), the other with an estimation of the relative concentration of the minerals as 'major', 'minor', and 'trace' (Chisonga et al. 2012). Based on these estimations, a reference value was obtained, helping to give some quantification to the estimation.

Table 4 shows the chemical composition of two groups of samples of queluzite from different mines. Samples collected by ICOMI came from the mines T-6, C-2 and T-20. Samples from F-12 were assayed by Chisonga et al. (2012), and divided into three rock types: Mn-silicate rock, meaning lenses rich in picrotephroite and rhodonite, a rhodochrosite marble, which is the queluzite with no picrotephroite and rhodonite, and a Mn-calcic marble, for the transition zone between the other two types.

For the exploration geologist looking for other manganese deposits in Amapá, it is important to observe the size of the garnets in exposures of oxidized ore. Garnets smaller than 2 millimeters, and the absence of quartz indicate a queluzite as the rock source. Greater garnets, quartz, and boxwork of silicates indicate a gondite.

2.7. Episodes of metamorphism

In Serra do Navio, the Serra do Navio Formation shows signs of three superposed episodes of metamorphism, with the first and the third being of regional extent, during which the rocks were folded and recrystallized up to the Amphibolite Facies of metamorphism. The second and intermediate metamorphic episode was thermal, and marked by the appearance of porphyroblasts, many of which preserve remnant minerals of the first episode of metamorphism.

The first regional metamorphic episode originated fold axis striking north-northeast, with a gentle plunge to the north, and with a foliation dipping to the east (Scarpelli and Horikava 2018). Staurolite, cordierite, and andalusite were formed in the quartz-silicate lithologies of the formation.

The intrusion of the Amapari granite, at the east of the district, is considered to be the source of the heat for the thermal metamorphism, as well as of the various masses of pegmatites intruded in the metasediments. The parallelism of flakes of muscovite of the pegmatites with the foliation of the intruded schists suggests that the last phases of the intrusion of the granite were contemporaneous with the initial phases of the second regional metamorphic episode.

During the thermal metamorphism, large porphyroblasts were formed in the carbonatic rocks, with diopside, tremolite and grossularite in the calcic and picrotephroite and rhodonite in the manganiferous ones (Fig. 15). The presence of a grossularite filling a fracture in diopside (Fig. 14) suggests that the process was not simple.

In the queluzites, rhodonite and picrotephroite occur as single crystals or forming clusters, not rarely cutting each other or another mineral. It is quite possible that the formation of these silicates depends on the ratio of silica with the manganese available for the reaction. Therefore, if there is an excess of silica, rhodonite is formed, with lower availability of silica leading to the formation of picrotephroite.

During the episode of thermal metamorphism, garnets grew into larger crystals, and porphyroblasts of staurolite, andalusite, and sillimanite (Fig. 16A, B, C) were formed in all the lithologies, with the exception of the carbonatic rocks and the gondites, being more abundant in the graphitic

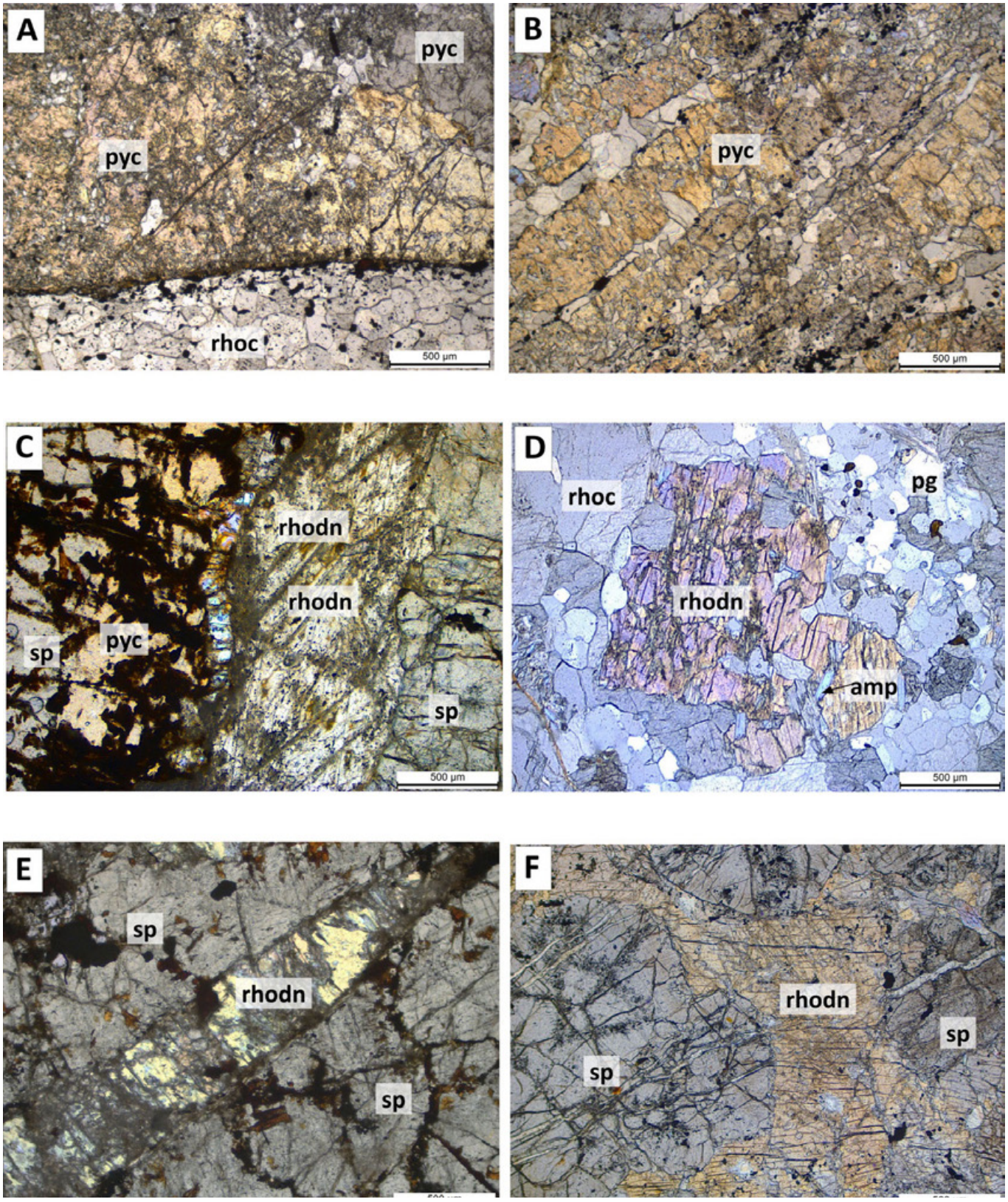

FIGURE 14. Porphyroblasts in the quartzose facies. (A) Regrowth of a grossularite garnet in a tremolite schist. The initial grossularite, marked by the dark blue line, has dark inclusions not observed in the area of regrowth, outlined by a yellow line. (B) Poikilitic almandine in a pocket of quartz in a biotite-quartz-plagioclase schist. (C and D) From the A-12 mine, large porphyroblasts of diopside are crossed by grossularite garnet. Views under uncrossed and crossed-nicols.

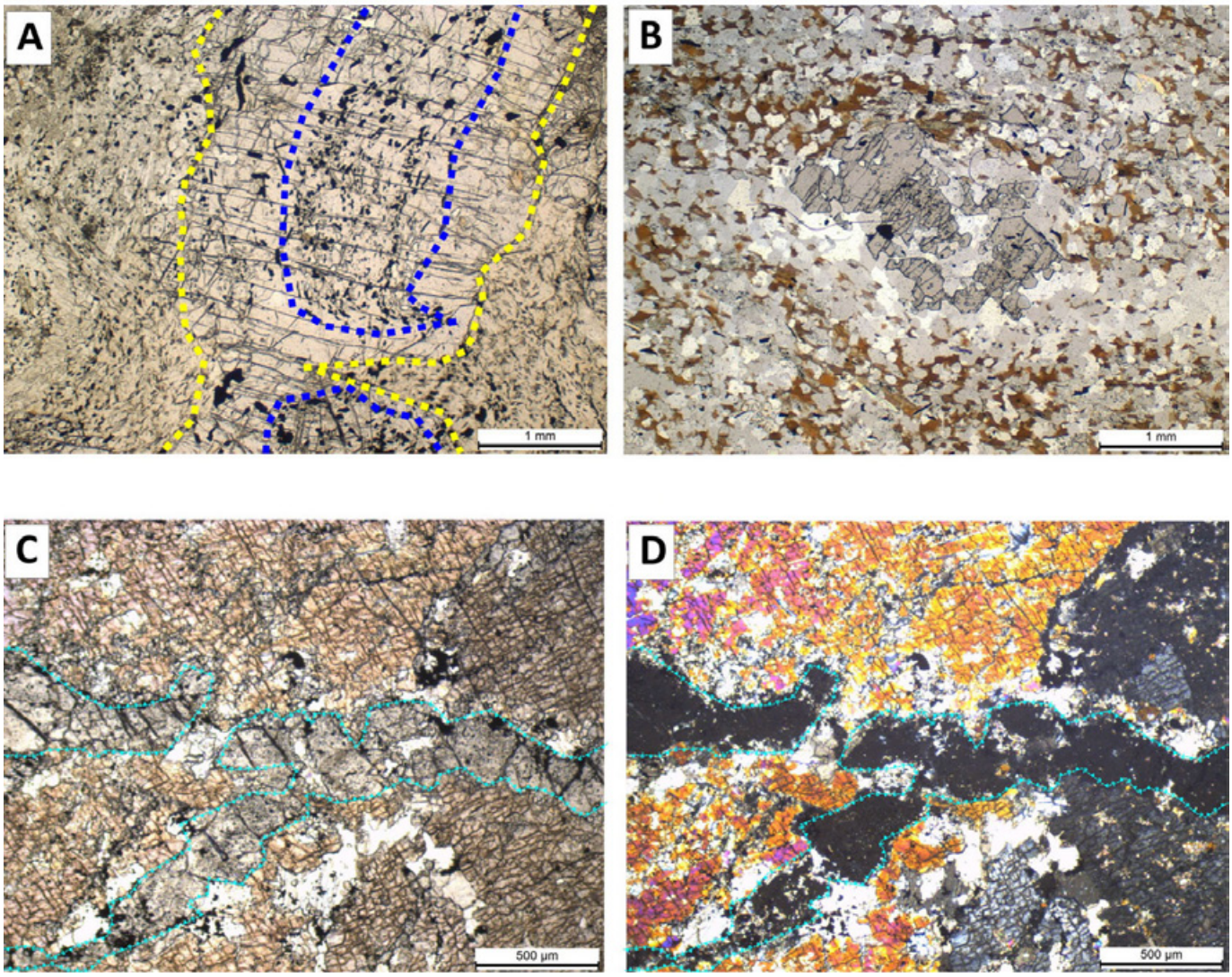

FIGURE 15. Porphyroblasts of the biotitic and graphitic facies. (A) From mine T-4, a quartz-biotite schist with cruciform twinned crystals of staurolite. (B) From mine T-4, porphyroblasts of andalusite with inclusions of graphite in a fine-grained quartz-feldspar-graphite schist. Some of the porphyroblasts show regrowth at their margins. (C) From mine C-1, crystals of sillimanite replace a mass of biotite in a quartz-biotite schist. (D) From mine T-20, porphyroblasts of cordierite in a quartz-plagioclase-biotite schist. These porphyroblasts of cordierite are rounded at their extremities.

schists. Andalusite predominates over staurolite in the three sedimentary facies and locally was partially replaced by staurolite by the edges. Cordierite is present in the biotitic facies (Fig. 16D), and, as well as andalusite and garnets, quite often preserve in their interior remnant minerals, such as biotite, staurolite, and graphite, showing the orientation developed during the first regional metamorphism (Fig. 17).

During the second episode of regional metamorphism, quartz, feldspars and micas recrystallized along the new foliation. Due to the tectonic sliding accompanying the development of the new foliation, some porphyroblasts were rotated, pressing adjacent micaceous minerals. When the porphyroblasts were moved, quite often areas of lower pressure appeared behind them or at their margins, becoming sites for the crystallization of quartz (Fig. 17D).

Sillimanite is a common accessory mineral in the silicate units of the formation, often seen in areas of stress and tectonism (Fig. 18). In these areas, it replaces other minerals, including andalusite, and may completely mask the rock. Occasionally, a wave of needles of sillimanite marks small shear zones. In Figure 19, quartz and clouds of sillimanite outline the path followed by a half of a broken garnet. While the half-garnet was being pushed ahead, quartz filled the open space left behind, and sillimanite was formed on the walls of the path of the half-garnet, where stress and friction were higher.

The shearing exposed at the T-6/T-4 and T-20 mines and marked by the chloritized orthoamphibolites in the Amapari River seems to have occurred during the final phases of the second regional metamorphic episode. It caused spread and weak retro-metamorphism, fracturing and displacements (Fig. 20), chemical replacements, and recrystallizations (Fig. 21).

Throughout the district, there are showings of light retrograde hydrothermalism (Fig. 22), contemporaneous with the final tectonic phases of the second regional metamorphic episode. They are typical of low-temperature action of fluids containing carbonates, silica, sulfur, and other elements. They are represented by narrow veinlets of quartz and/or calcite, some containing pyrite and with chlorite at their margins, and also by dissemination of fine-grained tourmaline. The presence of galena was observed in a quartzite. Chalcopyrite was seen in a few veins hosted in biotite schists. None of them suggest the presence of a metallic concentration of economic size.

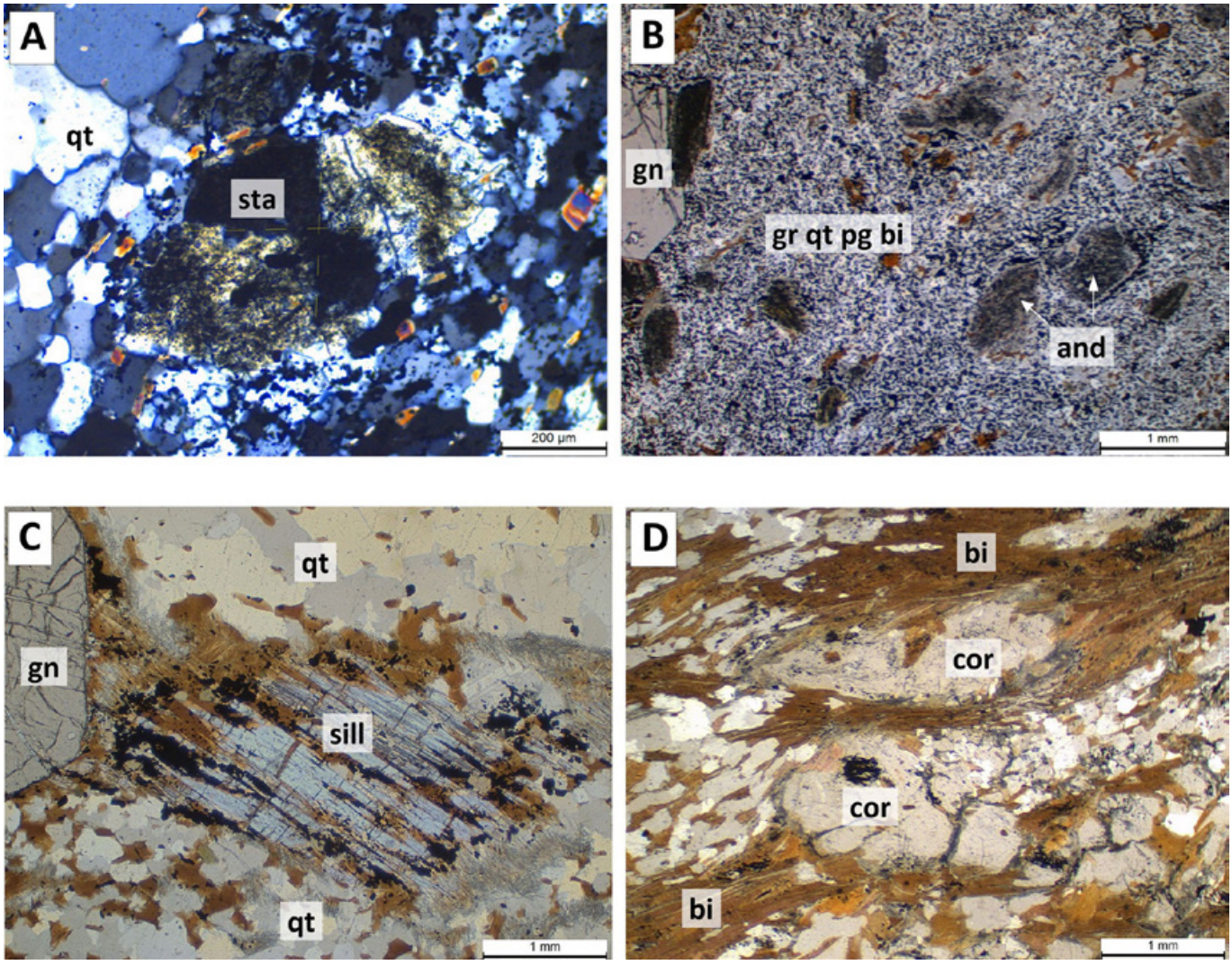

FIGURE 16. Porphyroblasts in queluzite. (A) From C-2 mine, a large picrotephroite with a straight face against mosaic textured rhodochrosite. (B) From C-2 mine, a picrotephroite with rhodochrosite filling spaces along planes of cleavage. (C) From A-12 mine, triple veining in an aggregate of spessartite. In contact with the garnet, picrotephroite appears at the left and rhodonite at the right. A younger and narrow vein of rhodonite cuts through the center, between rhodonite an picrotephroite. (D) From A-12 mine, a porphyroblast of rhodonite, with inclusions of rhodochrosite and crossed by an amphibole, is immersed in a mass of mosaic textured rhodochrosite with some plagioclase. A small group of crystals of albite appears at the upper right. (E) From A-12 mine, a narrow vein of rhodonite cutting through spessartite. (F) From C-2 mine, an irregular mass of rhodonite filling spaces between crystals of spessartite.

2.8 The Serra da Canga Formation

Only the base of the Serra da Canga Formation occurs in Serra do Navio (Scarpelli and Horikava 2017), concordantly covering the Serra do Navio Formation in the east of the area. The base of the unit is constituted by layers of cummingtonite schists and para-amphibolites. These two distinct lithologies differ in the nature and percentage of the amphibole they present, one with cummingtonite, and the other with hornblende. All amphibolites, by definition, have more than 50% of hornblende. These rocks differ from the Jornal orthoamphibolites for their clear sedimentary mineralogical banding, characterized by darker and lighter layers, and by the total absence of magnetite, when tested with a magnet (as it happens with basalts and ultramafic rocks, every orthoamphibolites presents magnetite as a minor component. The same occur with hornblende gneisses derived from these igneous rocks). Above these units, there are layers of metachert and biotite schist up to the top of the Serra do Veado, which presents the higher elevations of Serra do Navio. In four sites on this ridge, there are small accumulations of blocks of oxidized gondites. The exploration of these areas revealed that the gondites were associated with graphite-rich schist, in an up to four-meter-thick sequence. Their exploration indicated that they constitute low-tonnage resources of low-grade manganese oxide ore.

At the Serra da Canga, 15 kilometers to the east of Serra do Navio, the sedimentary sequence is complete. Above these gondites, there is a superposition of layers of metachert, quartzites, biotite schists, very narrow passages of graphitic schists and para-amphibolites, with interlayers of limestone in the lower part, of dolomites in the middle zone and of oxide iron formation (itabirites) at the top.

2.9. The Amapari granite and pegmatites

The Amapari granite is leucocratic and medium-grained, quartz-feldspathic, and with a dominance of muscovite over biotite. It contains occasional crystals of almandine garnet,

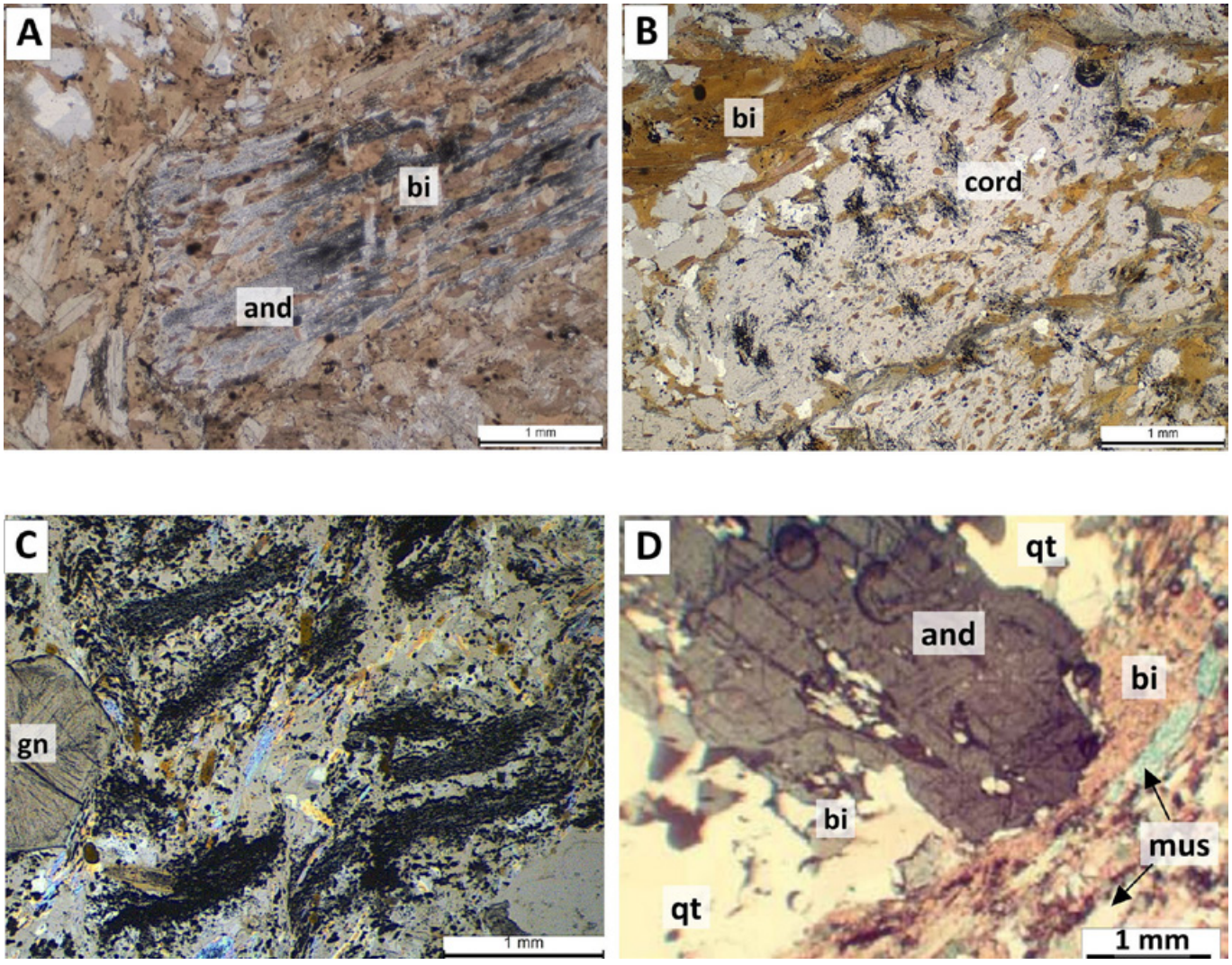

FIGURE 17. Evidence of superposition of the two regional metamorphic episodes. (A) From mine C-2, a porphyroblast of andalusite, with biotite filling cleavage planes, retains lines of fine-grained graphite formed during the first regional metamorphism. It is cross-cut by biotite formed during the second regional metamorphism. (B) From mine T-4, the photo is similar, showing a porphyroblast of cordierite, which during its growth incorporated small masses and lines of fine-grained graphitic schist, oriented to the upper left. The porphyroblast is oriented parallel to the foliation of the second regional metamorphic episode, which is oriented to the upper right. (C) From mine T-20, a fine-grained graphite schist, with layers oriented to the upper right, is disrupted and traversed by a more recent and discordant foliation created during the second regional metamorphic episode (D) From mine T-20, a biotitic schist shows an andalusite porphyroblast that rotated and smashed muscovite and biotite, becoming perpendicular to the foliation formed during the second regional metamorphic episode. New quartz crystallized in the spaces opened at the side of the porphyroblast.

and shows, near the contact with the metasediments, a weak foliation parallel to the contact.

On one occasion, two parallel two-kilometer-long lines of outcrops of a similar but coarser granite were found in the mine concessions, at the base of the Serra da Canga Formation, and were mapped as “syntectonic granite” (Scarpelli 1966). Later, when ICOMI opened caves to mine these masses, to produce railway ballast, it was verified that they are exposures of isolated masses of pegmatites, without significant lateral extension for the anticipated use.

Small bodies of pegmatite, with less than 0.5 meters of width fill fractures of the biotitic schists of the Serra do Navio Formation. They are similar but coarser than the Amapari granite. Quite often, they contain crystals of almandine garnet and fine-grained sillimanite, and tourmaline. Some of these pegmatites have the flakes of muscovite disposed parallel to the flakes of micas of the intruded schist, indicating, that the metamorphism of the schist is contemporaneous with that of the pegmatite.

2.10. Dikes and recent sediments

Triassic dikes of diabase oriented to north are common in the area. They are related to the Central Atlantic Magmatic Province (Marzoli et al. 1999). The larger reach nearly 50 meters of thickness. Throughout the area, the valleys are covered by recent sandy sediments.

3. The queluzites: an opportunity for reactivation of mining in Serra do Navio

The queluzites of Serra do Navio constitute important resources of manganese carbonates, and possibly also of manganese silicates, to supply the metallurgical industry, the

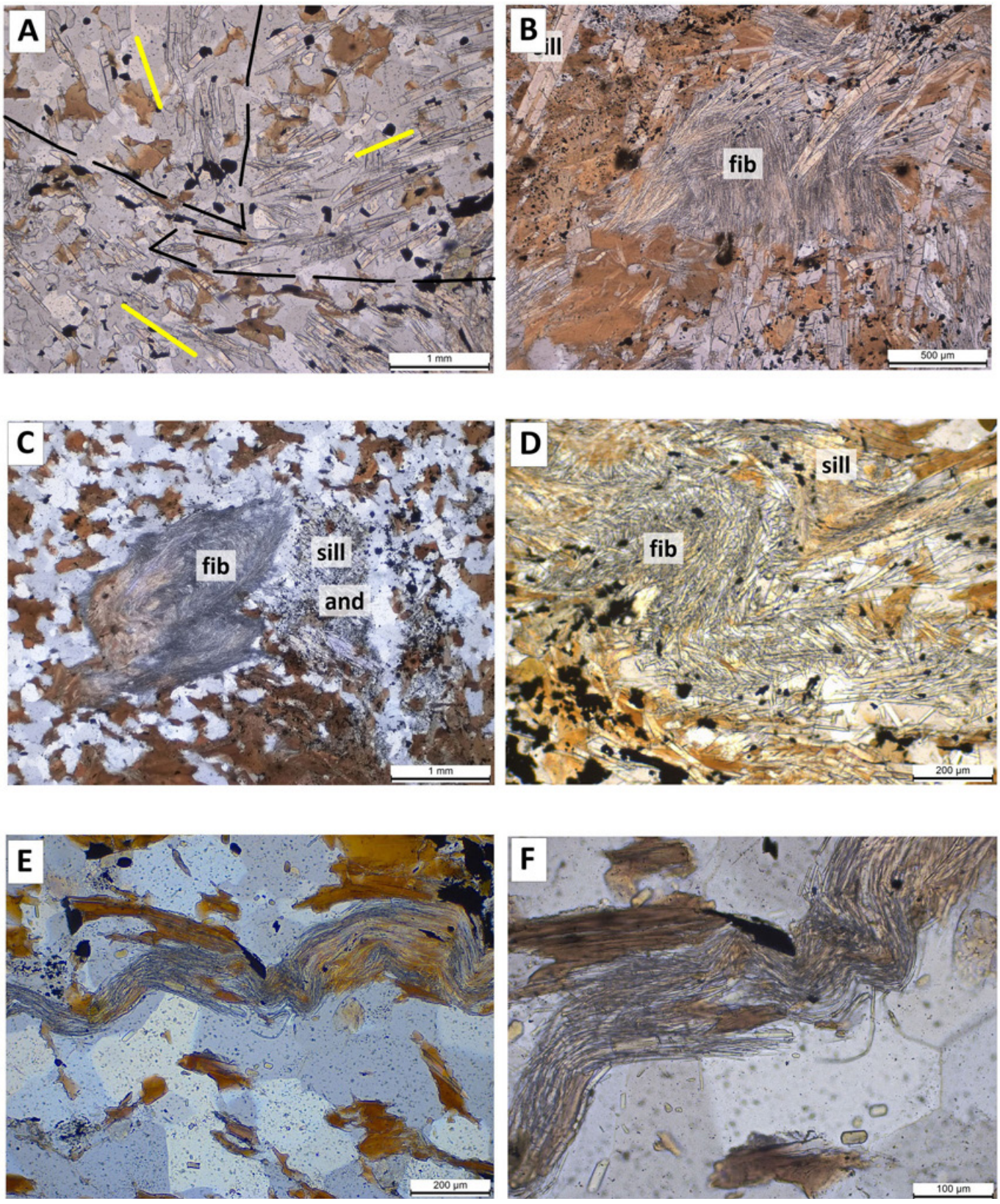

FIGURE 18. Sillimanite and fibrolite. (A) From mine C-1, a biotite-quartz-plagioclase schist of the quartzose facies presents clear sillimanite crystals, which appear with three different orientations, marking three tectonic sectors. At the upper right, they are oriented to the upper right; at the upper left, they point to the upper left; and at the lower half, they are oriented from left to right. It seems that these areas were rotated after the formation of the crystals. (B) From mine C-2, a schist of the biotitic facies presents sillimanite grown over biotite. At the center of the image, a large sillimanite (light gray) is replaced by bundles of fibrolite, which are in turn replaced by a few crystals of sillimanite (yellowish). (C) From mine C-2, at the left, bundles of fibrolite replace sillimanite which replaced biotite, while, at the right, sillimanite replace andalusite, both crossed by a quartz veinlet. (D) At mine C-5, crystals of sillimanite replacing biotite are partially replaced by fibrolite in an area bent by folding. (E and F) From mine T-6, a folded bundle of fibrolite crossing a biotite-quartz schist of the quartzose facies. At (F) it is possible to see bent crystals of fibrolite, what is never seen in sillimanite. Note the mosaic texture of the quartz.

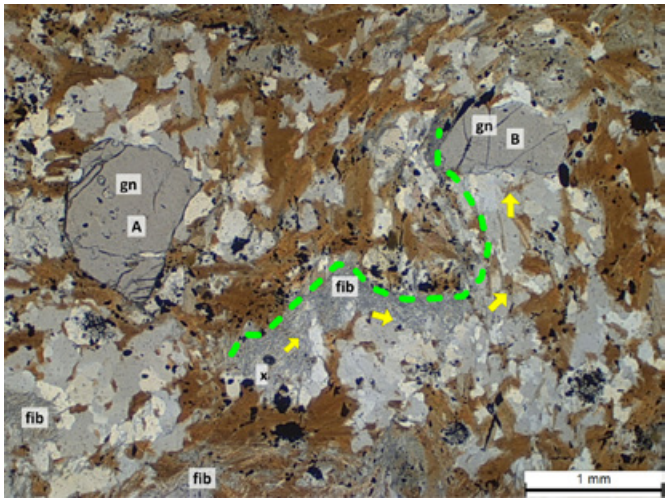

FIGURE 19. From mine C-5, during the second regional metamorphic episode, an almandine porphyroblast of a biotite schist was broken into two parts: A and B. Part A remained where it was, and part B was pushed ahead, along an irregular and curved track, which is indicated by the yellow arrows. While the half-garnet was moving, quartz crystallized in the space opened behind it. The moving half-garnet applied pressure on the rocks at its left-hand side, heating them, and leading to the crystallization of a continuous zone of fibrolites, the base of which is marked by the green line. In the 1-millimeter space between part A and the "x" site, where the fibrolite and the fresh quartz first appeared in the section, the part B moved above or below the plane of the section.

agriculture, the food industry and other needs. Obviously, their mining will depend on a careful study of the market and on the economic viability of the mining operation. This might not be for now, but the time will come.

If a mining project is considered attractive, it has to start with a geological exploration program, initially based on drilling, to obtain solid data on where are the better lenses of queluzites, their tonnages and their grades. Following, metallurgical test work has to be conducted on core samples, and after, galleries or caves have to be dug to collect bulk samples. A by-pass might be possible, with the use of the 6.000 tonnes of stockpiled crushed rhodochrosite ore obtained by ICOMI from F-12.

Size-wise, there should be much more than 40 million tonnes of fresh queluzite below the cover of weathered schists. This is the tonnage of manganese oxides that was mined. Just as a reference of potential, the few 16 holes that reached and cored the queluzite in the mined areas (Fig. 23) showed a resource estimated by ICOMI of up to 4,400,000 tonnes, in average assaying over 30% Mn (Costa 1997).

At this moment, rhodochrosite is more valuable than the manganese silicates, so, it is important to look where are the lenses with more rhodochrosite. If picrotephroite and rhodonite are considered 'impurities,' the exploration should prioritize the queluzites of the T-6, T-4 and T-20, which are mainly made of rhodochrosite, followed by the queluzite of the lower cyclothem of the A-13, C-10 and C-5.

Table 4 show that there is a large contrast among the percentages of rhodochrosite in the queluzites from the mines, being much greater at T-6, T-4, and T-20 than at C-2 and F-12 mines (Scarpelli 1966, Chisonga et al. 2012). Nevertheless, it should be considered that the F-12 has the silicates concentrated in identified layers of the deposit (Costa 1997, Chisonga et al. 2012). Actually, ICOMI produced clean rhodochrosite concentrates from F-12, avoiding the silicate-rich layers.

In the future, during the mining of queluzite, it should be considered that they occur in lenses, extending from hundreds of meters to over 1 kilometer, with thickness between a few to tens of meters. They occur in the upper portions of the layers of graphite schists that mark the upper facies of the sequence of the cyclothems. Structurally, the orebodies are close to vertical along the lineament of the T-11, to the T-6, T-4, and T20, which follow the large shear zone. To the North, throughout other mines, the regional structural geology is characterized by gentle folds, with a low angle of dip to the northeast (Fig. 23). This latter structure is more favorable to present large tonnages.

4. Discussion

4.1. Indicator minerals for pressure and heat

A point that deserves a comment, is the simultaneous occurrence of staurolite and andalusite in the silicate lithologies of the formation. Any explanation should pass by the acceptance that distinct lithologies react differently to pressure and heat, some resisting more, others less.

It is known that a hard, compact, layer of quartzite or chert resists more to tectonic deformation, preserving its layering. In contrast, a unit of metapelite in the same sequence will deform more easily, and form micaceous minerals, which help the slippage along the created foliation; in this way, they better disperse the heat and the pressure. These differences may explain the appearance of staurolite in the quartzites and metacherts and andalusite in the metapelites. At this point, it seems appropriate to consider that the andalusite, which appears as small and not idioblastic crystals in the compact and massive layers of quartzite, appears as large and idioblastic metacrystals in the more plastic units of graphitic facies, suggesting less resistance to their growth in the latter unit.

Another possibility for the different conditions of pressure and temperature could be the distance of the rock to the point where a shear zone or fault is applying high pressure, and the rock is becoming hotter.

Looking to sillimanite, here is a mineral that indicates localized pressure and heat. In some quartzites, it appears oriented along the lineation of the rock, being an indicator of slipping under stress and also along the foliation. In addition, it marks zones of shearing, and also shows areas of forceful movement of harder minerals, pressing and heating adjoining soft minerals (Figs. 18 and 19).

4.2. Sulfides of the queluzite and the Jornal Formation

Niccolite, gersdorffite, cobaltite and sphalerite are the only sulfides seen in the queluzites. This suggests a direct link between the queluzites and the mafic and ultramafic volcanic rocks which occur just below the base of the formation, now metamorphosed into the orthoamphibolites of the Jornal Formation.

The observation leads to the suggestion that manganese, together, with nickel, cobalt and zinc, may have been derived from the volcanic rocks, remaining in solution in the sea waters during the deposition of the formation, precipitating only in favorable lagoons of the graphitic facies of the cyclothems.

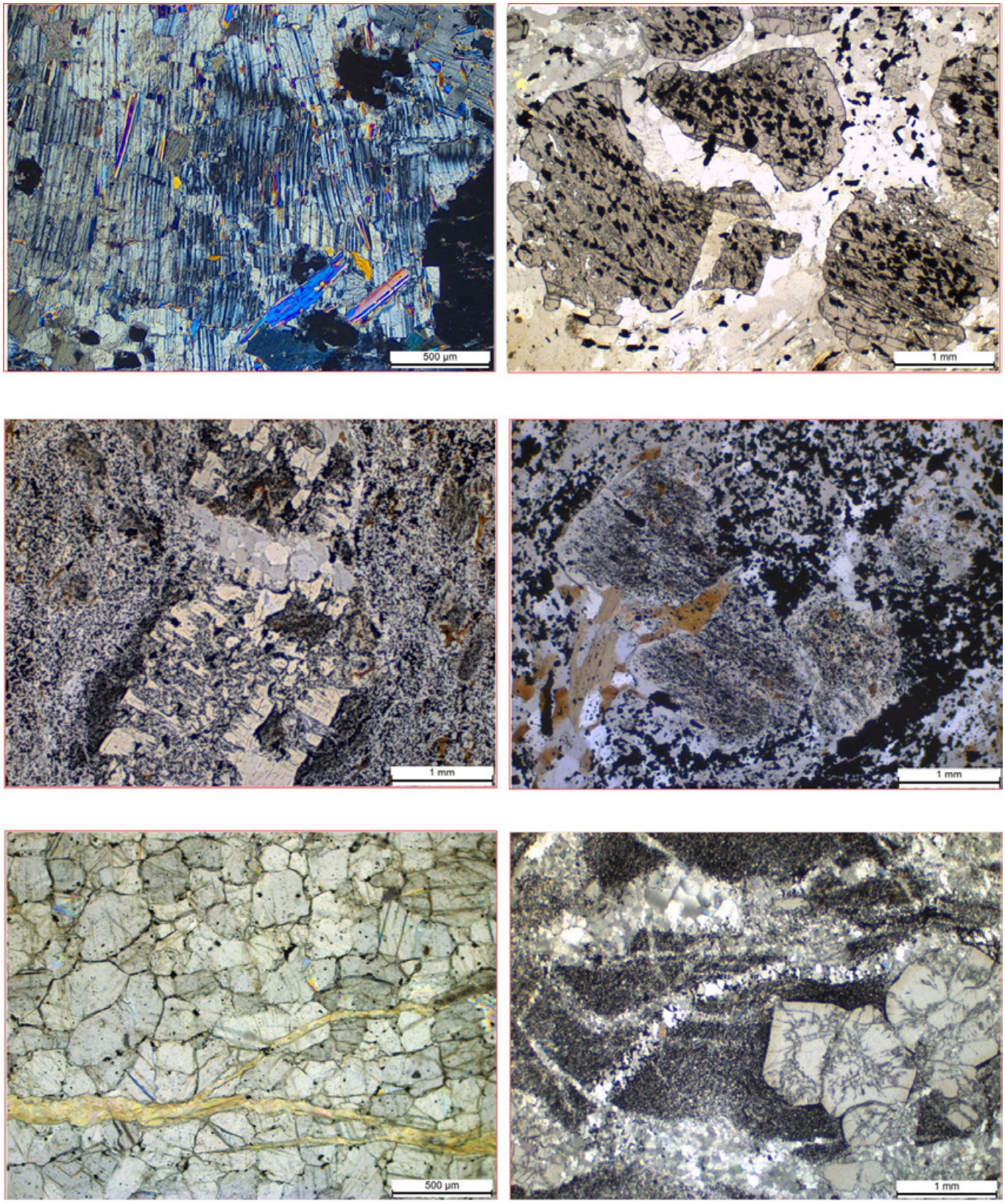

FIGURE 20. Fractures and veinlets formed during the second regional metamorphic episode. (A) From mine C-2, a rhodonite porphyroblast, broken and crossed by richterite, a manganoan amphibole. (B) From mine C-1, garnets containing oriented inclusions of graphite are broken, with some parts displaced, with the opened spaces filled with quartz and a chloritic mica, indicating the action of fluids. (C) From mine T-4, a broken porphyroblast of staurolite in a graphitic rock. Quartz crystallized in the opened space. (E) From mine C-2, one andalusite porphyroblast in a graphitic schist was broken, with the open spaces filled with quartz and biotite. The inclusions in the andalusite indicate the former foliation of the rock. (E) From mine T-9, mosaic-textured rhodochrosite-rich queluzite is fractured, with the fracture filled by zoisite. (F) From mine T-4, a queluzite with fine-grained rhodochrosite is fractured, with the fractures filled with coarse-grained rhodochrosite.

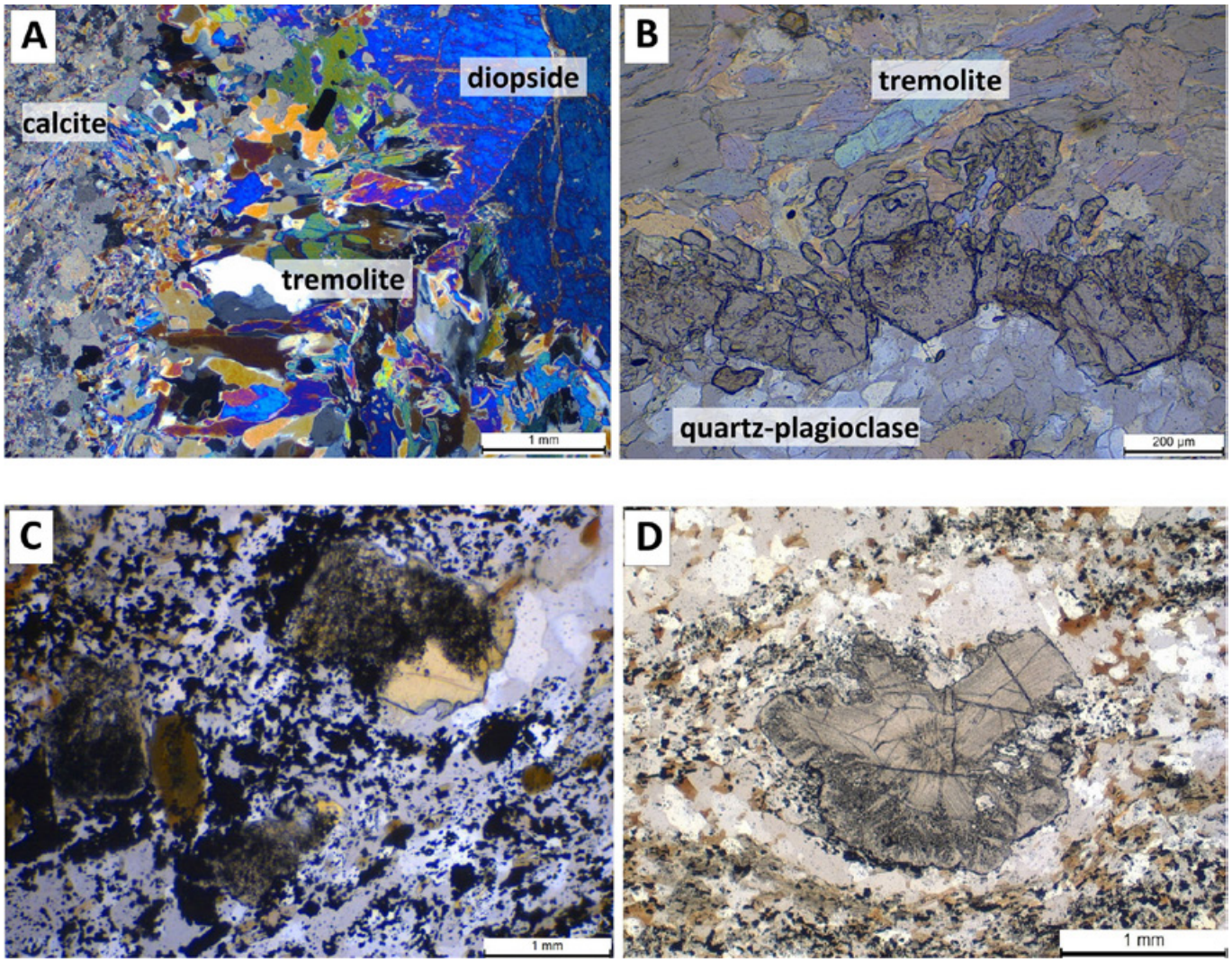

FIGURE 21. Chemical reactions and replacement during the second regional metamorphic episode. (A) From mine A-12, in the quartzose facies, a reaction between a marble and porphyroblasts of diopside led to the formation of tremolite crystals perpendicular to the contact. The tremolite crystals are greater at the contact with the diopside. (B) From mine C-1, grossularite garnets, on a layer at the contact of a quartz-plagioclase and a tremolite-rich bands, were partially replaced on the side at the contact with tremolite, but maintained their idioblastic form at the contact with quartz and plagioclase. (C) From mine T-4, in a graphitic schist, an inclusion-rich porphyroblast of staurolite regrew clean of inclusions at the contact with a quartz veinlet. (D) From mine T-6, in a biotitic schist, an almandine garnet appears surrounded by fresh quartz and was partially solubilized at its margins.

4.3. Future actions regarding the mining of the queluzites

It is highly recommended that the government sector that now controls the mineral rights represented by the concession keep it in good conditions, and, at the same time, make it available for bids for the exploration and mining of the resources of queluzite. As an example of the proposed model, the measures taken by CPRM to preserve mineral deposits discovered by the company, while looking for mining groups interested in their exploitation.

4.4. Final remarks

Chisonga et al. (2012) bring good laboratory information regarding the F-12 deposit, based on information obtained during a visit to the remaining cave of the F-12 mine in 2000 (when the mining had been completed, and most of the pits were under recovery and reforestation), and from the study of three drill holes and a geological section of the deposit. Therefore, as demonstrated in this paper, they examined only the upper part of the upper cyclothem, observing gondites, queluzites, graphite schists and biotite schists, missing the base of the biotitic facies, the complete quartzose facies, as well as the contacts and transition zones. Some remarks about their conclusions are as follow. (1) At F-12, the geological exploration and mining were limited to the upper part of the upper cyclothem, exposing queluzite, gondite, graphite schist and some biotite schist. The lithologies of the quartzose facies, including the calcic marbles, calc-schists, quartzites, and metacherts, were not available for observation. (2) Regarding the origin of the graphite, Chisonga et al. (2012) wrote: "*We, therefore, propose that graphite formed from sedimentary organic carbon and not by decarbonation of carbonates, as suggested by Scarpelli (1973).*" In fact, Scarpelli (1973) clearly wrote: *"…the graphitic facies is possibly the metamorphic product of a clayey sediment rich in carbonaceous material, which probably originated from organic matter accumulated with the clays…,"* and *"The free carbon did not originate*

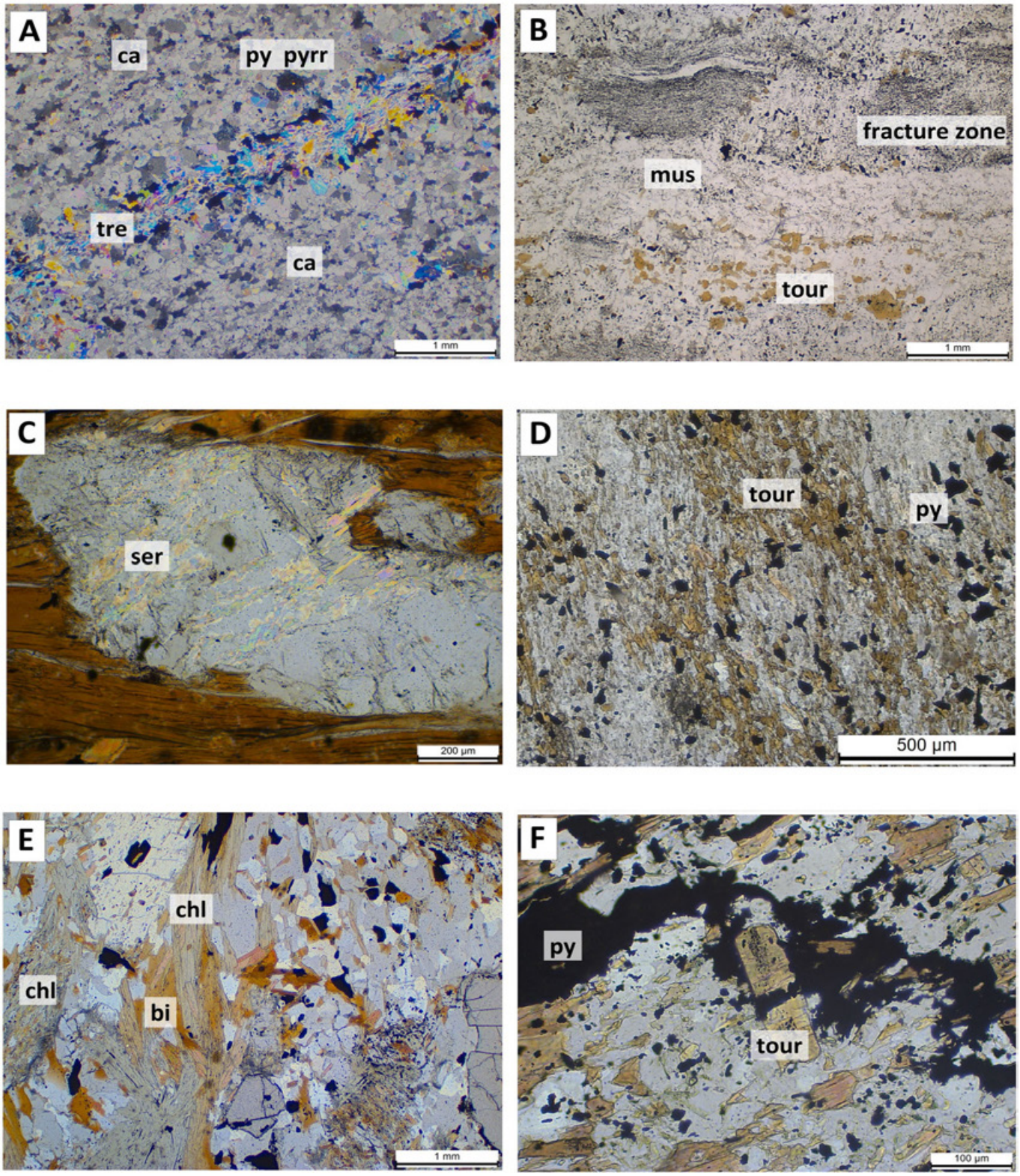

FIGURE 22. Late weak hydrothermalism. (A) From mine A-12, hydrothermal fluids penetrated along a fracture in a calcite-marble of the quartzose facies, leading to the formation of tremolite in the fracture, and of pyrite and pyrrhotite at the two margins of the tremolite zone. (B) From mine C-2, a layer of a weakly metamorphosed quartz-plagioclase schist of the quartzose facies was cut and altered by a transversal zone of fracture, marked by the presence of muscovite and by a close-by concentration of tourmaline. (C) From mine A-12, a partially sericitized porphyroblast of cordierite. (D) From mine T-20, a quartz-plagioclase schist of the quartzose facies with tourmaline and pyrite flanking nuclei of quartz-plagioclase. (E) From mine T-20, partial chloritization of biotite. (F) From mine T-20, an irregular vein of pyrite crossing a schist of the biotitic facies and a crystal of tourmaline.

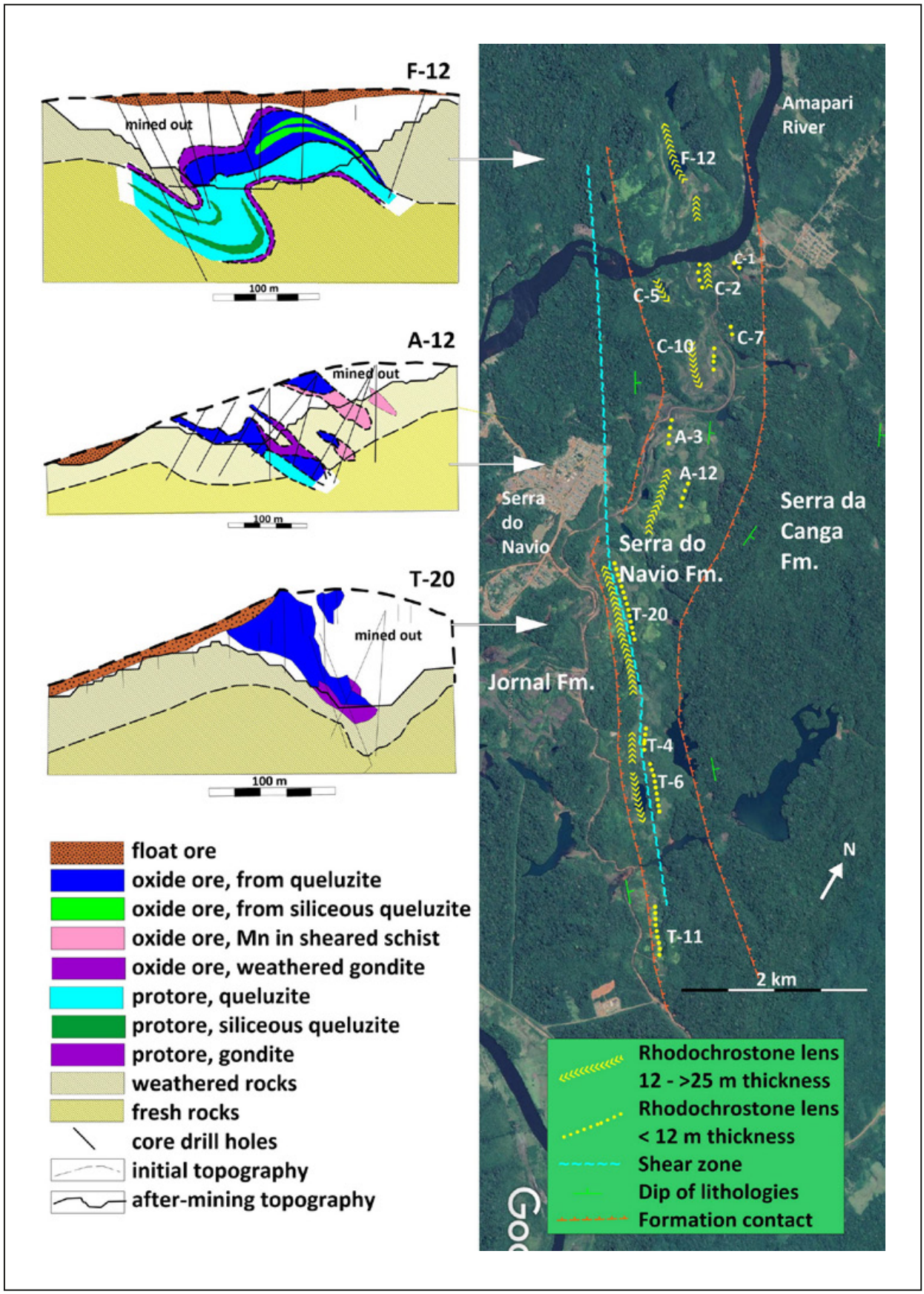

FIGURE 23. Drawn over a satellite image, the boundaries of the Serra do Navio Formation, and the location and identification of the thickest lenses of queluzites. On the left, sections of the F-12 (a thick queluzite with siliceous interlayers), A-12 (several lenses of queluzites) and T-20. All sections indicate a good potential of extension of the queluzite in depth. The section of T-20 represents the southern end of the mine, and the lens is thicker and goes deeper to the north. (These sections of F-12, A-12 and T-20 were taken from Costa 1997).

through decomposition of carbonates…". This was a repetition of the same argument first presented by Scarpelli (1966) on an intentionally cautious interpretation, considering that, in the sixties, Precambrian life had not been demonstrated yet. (3) As shown in this paper, the queluzite of the F-12 contains a few interlayers of manganiferous silicates (mostly picrotephroite, rhodonite and spessartite), between the parts rich in rhodochrosite. Chisonga et al. (2012) divided this queluzite into three parts, naming the transition zone between the two mentioned above as "Mn-calcite marble." Nothing wrong with the word "marble", but the word "calcite" is not appropriate, as there is no calcite in the rock, albeit the queluzites contain a few percent of calcium (Table 4). They could have written Ca-rhodochrosite marble, but we now suggest the use of queluzite as more appropriate. Calcite is quite common in the rocks of the quartzose facies, but Chisonga et al. (2012) have not studied the rocks of this facies. In silicate rocks of the other facies, calcite appears occasionally, in deformed areas, tiny veinlets together with quartz and a few iron sulfides. (4) Chisonga et al. (2012) interpreted the manganiferous silicate rock (Table 1), which is just a small part of the queluzites, as the "quartzose facies" of the formation. As they have not observed that facies, they have not considered the clean metachert, the limestones and the calc-silicate rocks that constitute the quartzose facies. (5) To interpret the origin of the deposit, Chisonga et al. (2012) considered that it was constituted by one single manganese-rich unit, deposited in a trench-like environment situated between two volcanic arcs, initially receiving volcaniclastic-argillaceous sediments, covered by pelites and then by manganese-oxides (diagenetically altered to carbonates) and, at the top, by carbonaceous shales. This environment never existed in Serra do Navio (Scarpelli 1966, 1973), as there are no volcaniclastic sediments there, and the deposition of organic-rich clays always preceded the deposition of manganese carbonates and continued for a short time just before the new subsidence that created the next cyclothem of the metamorphosed megacyclothem.

Acknowledgment

The author is deeply grateful to his wife, Lydia, for the support received throughout the years, and for those that worked and lived with him in the areas of ICOMI, in Serra do Navio, Santana and Rio de Janeiro. The pleasant and friendly environment maintained during the entire time was quite appealing, generating enthusiasm and friendship that is lasting through the years. Special thanks to Prof. Caetano Juliani, of the Instituto de Geociências da Universidade de São Paulo, for the friendly authorization given to the author, to use equipment of the university to obtain the microphotographs The author appreciates the comments of the Associate Editor Abidi Riadh and two JGSB anonymous reviewers.

Appendix A

Some definitions

Queluzite – A carbonate-rich metasedimentary rock similar to a limestone, or a dolostone, but with the carbonate being rhodochrosite, instead of calcite or dolomite. The word "queluzite" is well established in Brazil for the metamorphosed carbonatic sedimentary rock made mostly of rhodochrosite, as used by Guimarães 1935, Pires 1983, and others, for the rhodochrosite-rich metasediments of the manganese deposit of Morro da Mina, Minas Gerais. The word is also internationally known (Park et al. 1951; Dorr II et al. 1956).

Even so, this note is necessary due to the absence of the word "queluzite" in the Glossary of Geology (Neuendorf et al. 2011), which defines a sedimentary rock mainly composed of rhodochrosite as a "rhodochrostone", following Kim (1975), describing the mine of Janggun, South Korea. According to this author, the rock he described is not metamorphosed, contains clays and silica, and grades upwards and downwards to dolostones.

As the two names apply to rocks with the same chemical composition and sedimentary origin, it seems logical to use the word "rhodochrostone" for the sedimentary, and "queluzite" for the metamorphosed rock.

Cyclothem. The term, as used for the carbon-bearing sedimentary sequence of the Pennsylvanian period, in the USA, is a defined sequence of beds deposited during in a single sedimentary cycle. A megacyclothem is the vertical superposition of several cyclothems of the same type (Dunbar and Rodgers 1958; Duff et al.1967; Neuendorf et al. 2011).

Appendix B

The author activities in the area

The author worked in the manganese mines from 1961 to 1972, in mine geology and in local and regional exploration. During this period, many overtime hours were spent on petrographic studies which improved the understanding of the origin and the geology of the ores and their host rocks. From 1973 to 2006, he returned to the area on several occasions, and carried out regional geological exploration work for base metals, manganese, gold, iron, and chromium. As a result of the above and because of effective teamwork, the Tucano gold mine and the Amapari iron mine were discovered and opened (Scarpelli and Horikava 2017). During the early years of this century, he returned to the area to help ICOMI to solve and correct a problem with arsenic in Santana.

References

Ackerman F.L. 1948. Recursos minerais do Território Federal do Amapá. Rio de Janeiro, Imprensa Nacional, 30 p.

Barreto C.J.S., Lafon J.M., Rosa-Costa L.T, Dantas L. 2013. Paleoproterozoic granitoids from the northern limit of the Archean Amapá block (Brazil). Journal South American Earth Sciences, 45, 97-116. https://doi.org/10.1016/j.jsames.2013.02.005

Bellizia C.M. 1972. Paleotectónica del Escudo de Guayana. In: Conferencia Geológica Inter Guayanas, 9, Ciudad Guayana, Venezuela, 251-304.

Castro L.O. 1963. Study of the manganese ore deposit of the Serra do Navio District – Amapá, Brasil. Boletim da Sociedade Brasileira de Geologia,12(1-2), 5-35. Available on line at: http://boletim.siteoficial.ws/pdf/1963/12_1-2-1-34.pdf / (accessed on 7 July 2022).

Chisonga B.C., Gutzmer J., Beukes N.J., Huizenga J.M. 2012. Nature and origin of the protolith succession to the Paleoproterozoic Serra do Navio manganese deposit, Amapa Province, Brazil. Ore Geology Reviews, 47, 59-76. https://doi.org/10.1016/j.oregeorev.2011.06.006

Choubert B. 1973. Occurrences of manganese in the Guianas (South America) and their relation with fundamental structures. In: Unesco. Genesis of precambrian iron and manganese deposits:

proceedings of the Kiev Symposium, 20-25 August 1970. Paris, Unesco. p. 143-151.

Costa R.C. 1997. Exaustão das reservas remanescentes do Distrito Manganesífero de Serra do Navio. Private document prepared by Roberto Costa Eng., on behalf of ICOMI, presented to the DNPM (Departamento Nacional de Produção Mineral) during cessation of mining activities.

Dardenne M.A., Schobbenhaus C. 2001. Depósitos de manganês da Serra do Navio. In: Dardenne M.A., Schobbenhaus C. Metalogênese do Brasil. Brasília, Editora Universidade de Brasília, 392 p. Available on line at: https://rigeo.cprm.gov.br/handle/doc/1291 (accessed on 1 July 2022).

Dorr II J.V.N., Park Jr. C.F., Paiva G. 1950. Depósito de manganês do Distrito de Serra do Navio, Território Federal do Amapá. Boletim DNPM, 85, 7-80

Dorr II J.V.N., Park Jr. C.F., Paiva G. 1949. Manganese deposits of the Serra do Navio District, Territory of Amapa, Brazil. US Geol Survey Bulletin, 964-A, 1-51. https://doi.org/10.3133/b964A

Dorr II J.V.N., Coelho I.S., Horen A. 1956. The manganese ore deposits of Minas Gerais, Brazil. International Geology Congress, 20, Symposium on Manganese 3, 277-346.

Dunbar C.O., Rodgers J. 1958. Stratification, in principles of stratigraphy. New York, John Wiley & Sons, Inc. 356 p.

Duff P.McL.D., Hallam A., Walton E.K. 1967. Cyclic sedimentation Developments in Sedimentology 10. Elsevier Pub. Co.

Gault H.R. 1959. On the mineralogy and textures of ore samples N-57 to N-62 (ICOMI). Internal report of Bethelehem Steel to ICOMI, reporting studies of samples of the ores.

Gibbs A.K., Barron C.N. 1993. Geology of the Guiana Shield. Oxford, Clarendon Press, 1993, 246 p.

Guimarães D. 1935. Contribuição ao estudo da origem dos depósitos de minério de ferro e manganês do centro de Minas Gerais, Brasil. Boletim 8, SFPM-DNPM, 70 p.

Hoffmann I.B., Philipp R.P., Borghetti C. 2018. Geochemistry and origin of the Rhyacian tholeiitic metabasalts and meta-andesites from the Vila Nova Greenstone Belt, Guyana Shield, Amapá, Brazil. Journal of South American Earth Sciences, v. 88, 29-49. https://doi.org/10.1016/j.jsames.2018.07.009

João X.S.J., Carvalho J.M.A., Vale A.G., Frizzo S.J., Martins R.C. 1979. Projeto Falsino: relatório final, texto explicativo e mapas 1:100.000. Belém, DNPM/CPRM. Available on line at: https://rigeo.cprm.gov.br/handle/doc/9876 / (accessed on 7 July 2022).

Kim S.J. 1975. Rhodochrostone: a new sedimentary rock from the Janggun mine, Korea. Gwansan Jijir = Journal of the Korean Institute of Mining Geology, 8(2), 63-71.

Leinz V. 1948. Estudo genético do minério de manganês de Serra do Navio, Território do Amapá. Anais Academia Brasileira de Ciências 20(2). Available on line at: http://memoria.bn.br/DocReader/158119/5875 / (accessed on 8 July 2022)

Lima M., Montalvão R., Issler R., Oliveira A., Basei M., Araujo J., Silva G. 1976. Folha NA/NB.22, Macapá. Projeto Radam; MME-DNPM, Levantamento de Recursos Naturais, V-6, Geologia. Available on line at: https://biblioteca.ibge.gov.br/index.php/biblioteca-catalogo?view=detalhes&id=2100370 / (accessed on 8 July 2022).

Lima M.D., Henrique M.C., Linhares A.M., Vilhena S.M.P., Santos L.C.A.N. et al. 2008. Vila Serra do Navio: dossiê de tombamento. Brasília, IPHAN. 238 p.

Marvin U.B. 1956. Mineralogy of the manganese ores at Amapá, Brazil. Internal report to Bethelehem Steel to ICOMI, reporting analysis of samples of the massive ores.

Marzoli A., Renne P.R., Piccirillo E.M., Ernesto M., Bellieni G., De Min A. 1999. Extensive 200-million-year-old continental flood basalts of the Central Atlantic Magmatic Province. Science, 284(5414), 616-618. https://doi.org/10.1126/science.284.5414.616

Nagell R.H., Seara A.C. 1959. The geology and mining of the Serra do Navio manganese deposit, Amapá, Brazil. 5th Inter Guiana Geol. Conf. Georgetown; p 299-303

Nagell R.H. and Silva A.R. 1960. O carbonato de manganês como protominério no Distrito de Serra do Navio. XIV Cong. Soc. Bras. Geo., Brasília

Nagell R.H. 1962. Geology of the Serra do Navio Manganese District, Brazil. Bul Soc Econ. Geol. Vol. 57, 482-498

Neuendorf K.K.E, Mehl Jr. J.P. and Jakson J.A. 2011. Glossary of Geology 5th Edition. American Geosciences Institute, Virgínia, USA.

Park C.F., Dorr II J.V.N., Guild P. W., and Barbosa A.L.M.; 1951. Notes on the manganese ores of Brazil; Bull. Soc. Econ. Geologists, Econ Geology, vol 46, nº 1, 1-22

Pasquali J.Z. 1972. Expresión geoquímica superficial de la mineralización en el Distrito Minero de El Callao. 9th Inter Guiana Geol Conf., Ciudad Guayana, Venezuela; 443-451

Pires F.R.M. 1983. Manganese mineral paragenesis at the Lafaiete District, MG, Brazil. Anais da Academia Brasileira de Ciências, 55(3) 272-285

Ramos C.V. 1983. História do aproveitamento das jazidas de manganês da Serra do Navio, Vol. I - historical review 1943-1983. Prepared by ICOMI for free distribution, 223 p

Rosa-Costa L.T., Lafon J.M., and Delor C. 2006. Zircon geochronology and Sm-Nd isotopic study: Further constraints for the Archean and Paleoproterozoic geodynamical evolution of the southeastern Guiana Shield, north of the Amazonian Craton, Brazil. Gondwana Research, 10(3-4):277-300.

Rosa-Costa L.T., Chaves C.L. and Klein E.L. 2014. Geologia e Recursos Minerais da Folha Rio Araguari - NA.22-Y-B, Estado do Amapá, 1:250.000. Rio de Janeiro, CPRM.

Rodrigues O.B., Kosuki R., Coelho Filho A. 1986. Distrito Manganesífero de Serra do Navio, Amapá. In Principais Depósitos Minerais do Brasil. Vol II, Cap XIV, Ferro e Metais da Indústria do Aço. Departamento Nacional da Produção Mineral

Scarpelli W. 1961. "Determinação da picrotefroita". Internal report, ICOMI

Scarpelli W. 1966. Aspectos genéticos e metamórficos das rochas do Distrito de Serra do Navio. In: Inter Guiana Geological Conference, 6, Avulso 41, 37-56.

Scarpelli W. 1969. Preliminary geologic mapping of the Falsino River. In: Inter Guiana Geological Conference, 7, Paramaribo, Suriname. Verhandelingen van het Koninklijk Nederlands, 27, 125-129.

Scarpelli W. 1973. The Serra do Navio manganese deposit (Brazil). In: Unesco. Genesis of precambrian iron and manganese deposits. Proceedings of the Kiev Symposium; 217-228

Scarpelli W., Horikava H.H. 2017. Gold, iron and manganese in central Amapá, Brazil. Brazilian Journal of Geology, 47(4), 703-721. https://doi.org/10.1590/2317-4889201720170114

Scarpelli W., Horikava H.H. 2018. Chromium, iron, gold and manganese in Amapá an northern Pará, Brazil. Brazilian Journal of Geology, 48(3), 415-433. https://doi.org/10.1590/2317-4889201820180026

Silva A.R, Scarpelli W., Marotta C.A. 1963. Contribuição ao estudo dos protominérios de manganês do Distrito de Serra do Navio: território federal do Amapá. Boletim da Sociedade Brasileira de Geologia, 12(1-2), 37-48. Available on line at: http://boletim.siteoficial.ws/pdf/1963/12_1-2-35-46.pdf / (accessed on 8 July 2022)

Tassinari C.C.G., Macambira J.J.B. 2004. A evolução tectônica do Cráton Amazônico. In: Mantesso Neto V., Bartorelli A., Carneiro C.D.R., Neves B.B.B. (orgs.). Geologia do Continente Sul-Americano: evolução da obra de Fernando Flávio Marques de Almeida. São Paulo, Editora Beca. p. 471-485.

Valarelli J.V. 1966. Contribuição à mineralogia do minério de manganês de Serra do Navio, Amapá. Inter Guiana Geological Conference, 6, Avulso 41, 83-98.

Valarelli J.V. 1967. O minério de manganês da Serra do Navio, Amapá. PhD Thesis, Instituto de Geociências, Universidade de São Paulo, São Paulo, 149 p. https://doi.org/10.11606/T.44.2016.tde-09062016-151557

Winchell A.N., Winchell H. 1959. Elements of optical mineralogy: an introduction to microscopic petrography: part II. 4th edition. New York, Jonhn Wiley & Sons.